Fluid inclusion and stable isotope constraints on the origin of Wernecke Breccia and associated iron oxide – copper – gold mineralization, Yukon

Julie A. Hunt, Tim Baker, James Cleverley, Garry J. Davidson, Anthony E. Fallick, and Derek J. Thorkelson

Abstract: Iron oxide – Cu ± Au ± U ± Co (IOCG) mineralization is associated with numerous Proterozoic breccia bodies, collectively known as Wernecke Breccia, in Yukon Territory, Canada. Multiphase breccia zones occur in areas underlain by Paleoproterozoic Wernecke Supergroup metasedimentary rocks and are associated with widespread sodic, potassic, and carbonate alteration assemblages. Fluid inclusion data indicate syn-breccia fluids were hot (185–350 °C) saline (24–42 wt.% NaCl equivalent) NaCl–$CaCl_2$–H_2O brines. Estimates of fluid pressure vary from 0.4 to 2.4 kbar (1 kbar = 100 MPa). Carbon and oxygen isotopic compositions of breccia-related carbonates range from ~–11‰ to +1.5‰ (Pee Dee belemnite (PDB)) and –2‰ to 20‰ (Vienna standard mean ocean water (V-SMOW); $\delta^{18}O_{water}$ ~–8‰ to +15‰), respectively. $\delta^{13}C$ and $\delta^{18}O$ values for host Wernecke Supergroup limestone/dolostone vary from ~–2‰ to 1.6‰ and 12‰ to 25‰, respectively. Sulfur isotopic compositions of hydrothermal sulfides and sulfate vary from ~–12‰ to +13‰ and +8‰ to +17‰ (Cañon Diablo Troilite (CDT)), respectively. Syn-breccia biotite, muscovite, and actinolite have δD and $\delta^{18}O$ values of ~–141‰ to –18‰ and +7‰ to +12‰ (V-SMOW; $\delta^{18}O_{water}$ ~7‰ to 11‰), respectively. The Wernecke Breccias and the associated IOCG mineralization appear to have formed from largely nonmagmatic fluids — based on isotopic, fluid inclusion, and geological data. The emerging hypothesis is that periodic overpressuring of dominantly formational/metamorphic water led to repeated brecciation and mineral precipitation. The weight of overlying sedimentary rocks led to elevated fluid temperatures and pressures; fluid flow may have been driven by tectonics and (or) gravity with metals scavenged from host strata.

Résumé : Une minéralisation d'oxyde de fer – Cu ± Au ± U ± Co (IOCG) est associée à de nombreux amas de brèches datant du Protérozoïque, connus ensemble sous le nom de brèches de Wernecke, dans le Territoire du Yukon, Canada. Des zones de brèches à plusieurs phases se retrouvent dans les secteurs reposant sur des roches métasédimentaires du supergroupe de Wernecke (Paléoprotérozoïque) et ces zones sont associées à des assemblages étendus d'altération sodique, potassique et de carbonate. Des données sur des inclusions de fluides indiquent que les fluides contemporains des brèches étaient des saumures NaCl–$CaCl_2$–H_2O chaudes (185–350 °C) et salines (24–42 % poids équivalent NaCl). Des estimations de la pression des fluides varient de 0,4 à 2,4 kbar (1 kbar = 100 MPa). Les compositions isotopiques en carbone et en oxygène des carbonates reliés aux brèches varient respectivement de ~–11 ‰ à +1,5 ‰ (Pee Dee belemnite (PDB)) et –2 ‰ à 20 ‰ (Vienna standard mean ocean water (V-SMOW); $\delta^{18}O$ eau ~-8 ‰ à +15 ‰). Les valeurs $\delta^{13}C$ et $\delta^{18}O$ pour les dolomies/calcaires encaissants du supergroupe de Wernecke varient respectivement de ~–2 ‰ à 1,6 ‰ et de 12 ‰ à 25 ‰. Les compositions isotopiques du soufre des sulfures et sulfates hydrothermaux varient respectivement de ~–12 ‰ à +13 ‰ et de +8 ‰ à +17 ‰ (Cañon Diablo Troilite (CDT)). La biotite, la muscovite et l'actinote contemporaines de la brèche ont respectivement des valeurs δD et $\delta^{18}O$ de ~-141 ‰ à –18 ‰ et de +7 ‰ à +12 ‰ (V-SMOW; $\delta^{18}O$ eau :7 ‰ à 11 ‰). En se basant sur des données d'isotopes, d'inclusion de fluides et géologiques, il semblerait que les brèches de Wernecke et la minéralisation IOCG associée aient été formées à partir de fluides en grande partie non magmatiques. L'hypothèse résultante est que la surpression périodique de l'eau, surtout de formation/métamorphique, a conduit à

Received 15 May 2011. Accepted 31 May 2011. Published at www.nrcresearchpress.com/cjes on 21 September 2011.

Paper handled by Associate Editor Anthony Harris.

J.A. Hunt. Yukon Geological Survey, 102-300 Main St, Whitehorse, YT, Canada, Y1A 2C6, and School of Earth Sciences, James Cook University, Townsville, Queensland, 4811, Australia; ARC Centre of Excellence in Ore Deposits (CODES), University of Tasmania, Private Bag 79, Hobart, TAS, 7001, Australia.
T. Baker. School of Earth Sciences, James Cook University, Townsville, Queensland, 4811, Australia and Geological Survey Branch, Primary Industries and Resources, SA, 4-101 Grenfell Street, Adelaide, South Australia, 5000, Australia.
J. Cleverley. School of Earth Sciences, James Cook University, Townsville, Queensland, 4811, Australia and CSIRO Exploration and Mining, AARC, 26 Dick Perry Avenue, Kensington, West Australia, 6151, Australia.
G.J. Davidson. ARC Centre of Excellence in Ore Deposits (CODES), University of Tasmania, Private Bag 79, Hobart, TAS, 7001, Australia.
A.E. Fallick. Scottish Universities Environmental Research Centre, Rankin Avenue, East Kilbride, Glasgow, G75 0QF, Scotland.
D.J. Thorkelson. Earth Sciences, Simon Fraser University, Burnaby, BC V5A 1S6, Canada.

Corresponding author: Julie A. Hunt (e-mail: julie.hunt@utas.edu.au).

beaucoup de bréchification et de précipitation de minéraux. Le poids des roches sédimentaires sus-jacentes a mené à des températures et à des pressions élevées dans les fluides; les fluides peuvent avoir été poussés à couler par tectonisme et (ou) par gravité et contenir des métaux récupérés des strates hôtes.

[Traduit par la Rédaction]

Introduction

Numerous Proterozoic breccia bodies, collectively known as Wernecke Breccia, occur over large areas in the north-central Yukon Territory, Canada (Fig. 1; e.g., Bell and Delaney 1977; Archer et al. 1977; Bell 1978; Bell, 1986*a* and 1986*b*; Thorkelson 2000; Hunt et al. 2005). They are associated with extensive metasomatic alteration assemblages and significant, but little studied, iron oxide – copper ± gold ± uranium ± cobalt (IOCG) mineralization, which because of the low grade of metamorphism represents some of the best preserved examples of Proterozoic IOCG mineralization in North America. The scale of brecciation and alteration is similar to that in other large scale Proterozoic breccia provinces, including those in Australia that host the Ernest Henry (167 Mt @ 1.1% Cu, 0.54 g/t Au: Ryan 1998) and Olympic Dam (2000 Mt @ 1.6% Cu, 0.6g/t U_3O_8, 0.6 g/t Au: Reynolds 2000) deposits. Although many IOCG districts are characterized by brecciation and mineralization that is intimately related to magmatism from which ore fluids were sourced (e.g., Hitzman 2000; Sillitoe 2003) and (or) that provided heat to drive fluid circulation (e.g., Barton and Johnson 1996, 2000), a clear relationship with magmatic rocks or processes is not evident in the Wernecke Mountains.

One of the key aims of this study was to gain insight into the composition and source(s) of fluid(s) that formed IOCG mineralization and related breccias in the Wernecke Mountains. Six prospects were selected for analysis (Slab, Hoover, Slats-Frosty, Slats-Wallbanger, Igor, and Olympic; Figs. 1, 2) based on their varied stratigraphic locations within host Wernecke Supergroup strata, their association with extensive sodic or potassic metasomatic alteration assemblages, and the accessibility of drill core for study. This paper presents the results of fluid inclusion and stable isotope (C, O, S, and D) analyses for the six prospects and discusses how these results constrain possible fluid compositions and sources. Detailed descriptions of the prospects were presented in Hunt et al. (2005), and this information is presented only briefly here.

Regional geologic setting

Bodies of Proterozoic Wernecke Breccia, from 0.1 to 10 km^2, occur over large areas of the north-central Yukon Territory that are underlain by Paleoproterozoic rocks made up of Wernecke Supergroup, Bonnet Plume River Intrusions, and the informally named "Slab volcanics" (e.g., Gabrielse 1967; Delaney 1981; Bell, 1986*b*; Thorkelson 2000). The Wernecke Supergroup is a thick package of dominantly marine metasedimentary rocks that has been divided, from base to top, into the Fairchild Lake, Quartet, and Gillespie Lake groups (Fig. 2; e.g., Delaney 1981; Thorkelson 2000). The Fairchild Lake Group is at least 4 km thick and made up dominantly of fine-grained sandstone and siltstone, and minor limestone. These rocks are overlain by the Quartet Group, an ~5 km thick package of carbonaceous to calcareous fine-grained siltstone and sandstone. Transitionally, overlying the Quartet Group, and forming the upper part of the Wernecke Supergroup, is the ~4 km thick Gillespie Lake Group, made up largely of dolostone. Volumetrically, minor mafic to intermediate narrow dikes and sills and small stocks of the Bonnet Plume River Intrusions occur in the area underlain by Wernecke Supergroup (Thorkelson 2000; Thorkelson et al. 2001*a*). Earlier work (e.g., Thorkelson 2000; Thorkelson et al. 2001*a*) suggested that the Bonnet Plume River Intrusions crosscut the Wernecke Supergroup; however, recent detrital zircon data indicate that the Wernecke Supergroup rocks are significantly younger than the Bonnet Plume River Intrusions (Furlanetto et al. 2009). Further work needs to be carried out to resolve this relationship. Intermediate composition Slab volcanics also occur in this area; however, they are preserved only as clasts within Wernecke Breccia that was emplaced into upper Fairchild Lake Group rocks, and it is not clear if they are a local unit within Wernecke Supergroup or a separate unit that overlies it (Thorkelson 2000; Laughton 2004; Hunt et al. 2005). Wernecke Supergroup rocks were deformed and metamorphosed to greenschist facies during the Paleoproterozoic Racklan Orogeny. The timing of emplacement of the Bonnet Plume River Intrusions and Slab volcanics with respect to the orogeny is not clear (Thorkelson 2000). The absolute age of the Racklan Orogeny also is not known; however, it is constrained by crosscutting relationships to be, at least in part, older than Wernecke Breccia (i.e., Wernecke Breccia locally contains clasts of deformed Wernecke Supergroup: Thorkelson 2000). Crosscutting relationships observed to date indicate that Wernecke Breccia was formed syn- to post-deformation after peak metamorphism (Thorkelson 2000; Brideau et al. 2002; Hunt et al. 2005).

Wernecke Breccia is confined to areas of Wernecke Supergroup and is made up largely of clasts of the supergroup in a matrix of rock flour and hydrothermal precipitates; locally the breccia contains abundant clasts of Bonnet Plume River Intrusions and Slab volcanics (Thorkelson 2000; Hunt et al. 2002, 2005; Hunt 2005). Extensive sodic and potassic metasomatic alteration assemblages are spatially associated with the breccias and are overprinted by a carbonate alteration assemblage. Sixty five breccia occurrences are known, and all are associated with iron oxides and sulfides that occur as disseminations and veins within the breccia and surrounding Wernecke Supergroup rocks and locally as breccia infill (e.g., Archer et al. 1977; Archer and Schmidt 1978; Bell 1978, 1986*a*; Yukon MINFILE 2008). The Wernecke Breccias are included in the iron oxide – copper – gold class of deposits and were part of the original review of characteristics of this deposit type by Hitzman et al. (1992).

In the Slab area, breccia occurs in the upper part of the Fairchild Lake Group within a sequence of calcareous meta-

Fig. 1. Location of study area, distribution of Wernecke Supergroup and Wernecke Breccia plus location of breccia-associated IOCG prospects included in this study (modified from Thorkelson, 2000).

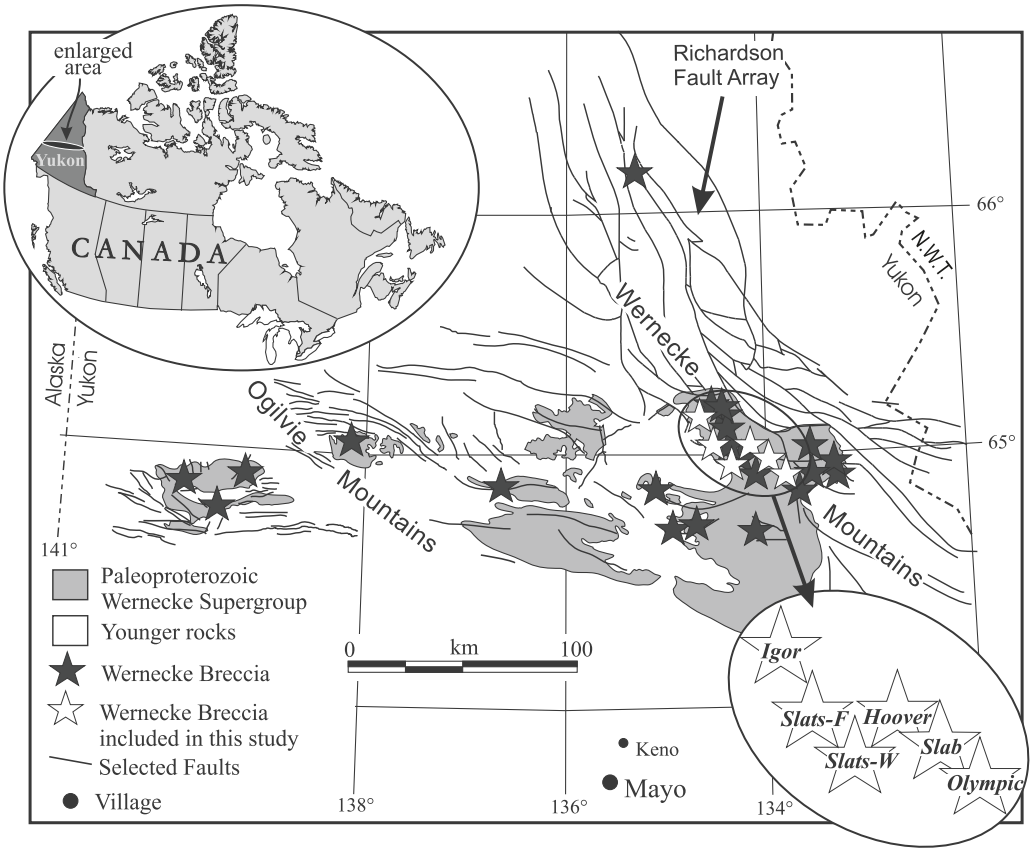

Fig. 2. Approximate stratigraphic position within the Wernecke Supergroup for IOCG prospects included in this study. *Slats-F* = Slats-Frosty; *Slats-W* = Slats-Wallbanger.

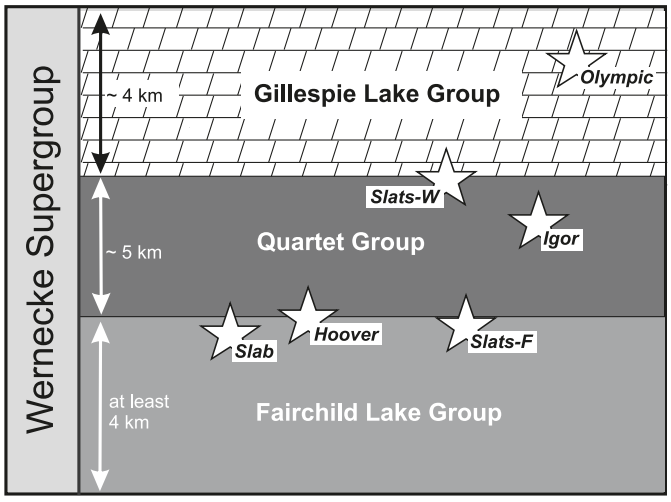

siltstone, minor limestone, and halite-facies metaevaporites (Fig. 2). Numerous and large clasts of Slab volcanics occur locally within the breccia (e.g., Delaney 1981; Thorkelson 2000; Hunt et al. 2005). Bonnet Plume River Intrusions outcrop locally in the Slab area. In the Hoover area, breccia bodies are in calcareous metasiltstone and carbonaceous shale/slate at the transition from Fairchild Lake Group to Quartet Group; minor amounts of Bonnet Plume River Intrusions occur in this area. In the Slats region, breccia occurs in two areas known informally as "Frosty" and "Wallbanger". Wallbanger is located about 4 km south-southeast of Frosty (Slats-W and Slats-F in Fig. 1). Breccia occurs within upper Fairchild Lake Group calcareous metasiltstone and phyllite in the Frosty area and within transitional Quartet Group to Gillespie Lake Group interlayered calcareous metasiltstone, shale, and dolostone in the Wallbanger area; Bonnet Plume River Intrusions occur in both areas. At Igor, breccia occurs within calcareous to carbonaceous metasiltstone and shale (Norris 1997) that are interpreted to be part of the Quartet Group. Breccias in the Olympic area were emplaced into locally stromatolitic Gillespie Lake Group dolostone in the upper part of the Wernecke Supergroup (Thorkelson 2000). Minor amounts of Bonnet Plume River Intrusions diorite and anorthosite occur as clasts in the breccia.

The age of brecciation is considered by Thorkelson (2000) and Thorkelson et al. (2001*b*) to be ca. 1595 Ma, based on a U–Pb date of 1595 $^{+8}_{-5}$ Ma on hydrothermal titanite from a sample of breccia matrix. It should be noted that there is a significant difference in age between Wernecke Breccia and Bonnet Plume River Intrusions (i.e., ca. 1710 Ma versus ca. 1595 Ma). The age of the Slab volcanics remains unknown, despite several attempts to date these rocks, but they must be older than Wernecke Breccia since they occur as clasts in several breccia bodies.

Each phase in the development of a breccia complex was probably multistage and overlapped other stages (Delaney

1981). However, broad paragenetic sequences were established for the breccia occurrences based on crosscutting relationships (Hunt et al. 2005). In general, there is an overall trend of (1) metasomatic alteration assemblages (sodic or potassic) that overprint greenschist-facies metamorphic mineral assemblages, (2) early stage brecciation accompanied by abundant magnetite ± hematite alteration, (3) a main phase of brecciation accompanied by hematite and chalcopyrite–pyrite ± magnetite, and (4) syn- to post-breccia carbonitization (calcite, ankerite–dolomite, siderite) ± pyrite, chalcopyrite, hematite, magnetite. At Igor, syn- to post-breccia barite veins are locally abundant in addition to carbonate veins.

The Wernecke Breccia IOCG prospects occur in a fairly remote area of northern Canada and, as such, have not received a great deal of study. However, ongoing exploration for copper, gold, and uranium is occurring in this region. Of the six prospects in this study, Slab and Igor have been explored the most extensively. A resource of 20 million tons of 0.35% Cu and 0.17 g/t Au has been outlined for Slab (Thorkelson et al. 2003). Significant results for Igor include 140 m of 0.76% Cu, 0.05 g/t Au and 0.042% U_3O_8 that contains 7 m of 7.37% Cu, 0.33 g/t Au, and 0.417% U_3O_8 (Cash Minerals, News Release January 23, 2008, www.cashminerals.com).

Fluid inclusion studies

Fluid inclusion petrography was carried out on quartz-, calcite-, fluorite-, or barite-bearing samples of Wernecke Breccia or associated veins at each prospect. The fluid inclusions examined were chosen because they are interpreted, based on paragenetic relationships (Hunt et al. 2005), to have formed during brecciation; examples are shown in Fig. 3. There is evidence in some of the Wernecke Breccia bodies that suggests the presence of overprinting hydrothermal systems, for example a 1383 Ma U–Pb rutile date reported in Thorkelson et al. (2001*a*); thus, we cannot entirely rule out the possibility of effects from younger fluids on fluid inclusions and isotopes. However, similar temperature and pressure results (see later in the text) suggest this is unlikely.

Fluid inclusion paragenesis was established using the criteria for primary, pseudosecondary, and secondary inclusions outlined in Roedder (1984). Three types of inclusions were identified on the basis of phases present at room temperature: (1) liquid plus vapor ± opaque (L + V); (2) liquid plus vapor plus halite (L + V + H); and (3) L + V + H plus opaque. Within each sample and within each of these inclusion types the phase ratios were consistent and had similar shapes and, therefore, could be treated as fluid inclusion assemblages (cf. Goldstein and Reynolds 1994).

Fluid inclusion microthermometry was performed on a Linkam, gas-flow heating–freezing stage at James Cook University, Townsville, Queensland, Australia. The stage was regularly calibrated using synthetic fluid inclusion standards having known phase transitions at –56.6 and 0.0 °C. During calibrations, the temperatures indicated by the thermocouple were within 0.2 °C of the standards. In each sample, all freezing experiments were carried out before the sample was heated. Salinity (wt.% NaCl equivalent (equiv.)) was estimated using the methods of Vanko et al. (1988) and Zwart and Touret (1994) and the program FlinCalc (J. Cleverley, written communication, 2003), which uses information from Zhang and Frantz (1987) and Brown (1998). Fluid inclusion results are summarized in Table 1 and given in more detail in the following section and in Hunt (2005).

Results of fluid inclusion studies

Slab area: Euhedral quartz from the matrix of Wernecke Breccia in the Slab area contains clusters of primary fluid inclusions. At room temperature, the inclusions contain liquid (70%–90%), vapor (5%–10%), and halite. Rarely, they contain a red mineral that is interpreted to be hematite. During freezing experiments, the formation of brown ice was observed in all inclusions, and initial melting temperatures (T_{fm}) were below –50 °C. Final ice-melting temperatures ($T_{m(ice)}$) ranged from –50 to –36 °C. In heating experiments, homogenization occurred via halite dissolution ($T_h = T_{h(s)}$) between 226 and 245 °C; homogenization of the vapor bubble ($T_{h(v)}$) occurred between 154 and 175 °C (Fig. 4; Table 1). Salinity of fluid in the inclusions is about 42 wt.% NaCl equiv., and the Na:Ca ratio is ~1.4 (Fig. 4; Table 1).

Hoover area: Quartz grains from Wernecke Breccia clasts in the Hoover area contain trails of secondary fluid inclusions that are interpreted to relate to syn-breccia fluids. At room temperature, most of the inclusions contain liquid (80%–90%) and vapor (10%–20%); one inclusion contains liquid (90%–95%), vapor (5%–10%), and halite. In freezing experiments, the formation of ice was observed in all inclusions; T_{fm} was below –50 °C and $T_{m(ice)}$ ranged from –34 to –25 °C (Table 1). Hydrohalite ($NaCl.2H_2O$) was observed in two L + V inclusions and melted at –1 and +1 °C ($T_{m(hh)}$, Table 1). Na:Ca ratios for these two inclusions are 0.4 and 0.7 (Table 1). Salinity for L + V inclusions ranges from 26 to 32 wt.% NaCl equivalent. The salinity of the L + V + H inclusion is 38 wt.% NaCl equiv., and the Na:Ca ratio is ~1.2. During heating experiments, L + V inclusions homogenized by vapor bubble disappearance between 153 and 172 °C. In the L + V + H inclusion, final homogenization occurred by halite dissolution at 188 °C.

Slats-Frosty area: Fluorite from a syn-breccia ferroan dolomite–fluorite–pyrite–chalcopyrite vein contains fracture-parallel trails of pseudosecondary fluid inclusions that are interpreted to relate to syn-breccia fluid. At room temperature, the inclusions contain liquid (90%–98%) and vapor (2%–10%) ± solid. Solids are halite, hematite, and black opaques. The formation of brown ice was observed in all fluid inclusions during freezing, T_{fm} was below –50 °C, and $T_{m(ice)}$ was between –35 and –23 °C (Table 1). Hydrohalite was observed in two L + V inclusions and in most L + V + solid inclusions; $T_{m(hh)}$ ranged from –22 to 3 °C. Salinity is between 24 and 32 wt.% NaCl equiv., and Na:Ca ratios vary from 0.8 to 1.6 (Table 1; Fig. 4). Daughter phases homogenized at higher temperatures than vapor in all inclusions (i.e., $T_h = T_{h(s)}$). Homogenization of the vapor bubble occurred between 68 and 160 °C (Table 1).

Igor area: Barite from Wernecke Breccia matrix in the Igor area contains clusters of small fluid inclusions that are interpreted to be primary (i.e., syn-breccia). At room temperature, the inclusions contain liquid (90%–95%) plus vapor (5%–10%). Phase changes were difficult to observe because of the small size of inclusions and the cloudiness of the barite. Only one initial melting temperature of –77 °C was recorded. $T_{m(ice)}$ ranged from –54 to –50 °C. Hydrohalite was

Fig. 3. Examples of fluid inclusions: (*a*) fluid inclusions containing L + V + H, (*b*) fluid inclusion containing L + V + H + h, (*c*) trails of secondary fluid inclusions parallel to fractures within quartz, and (*d*) L + V fluid inclusions in fluorite. L, liquid; V, vapor; H , halite; h, hematite.

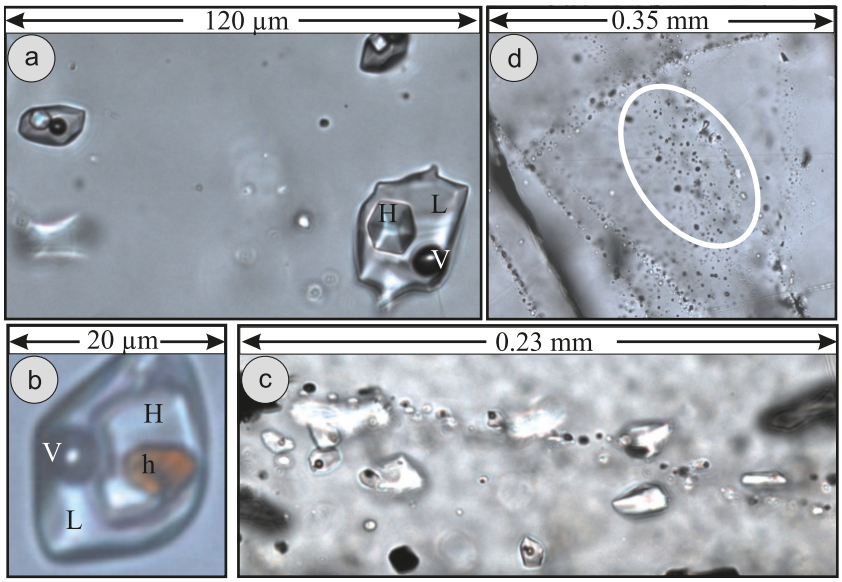

observed in one inclusion and melted at –26 °C. This inclusion has a salinity of 34 wt.% NaCl equiv. and a Na:Ca ratio of 0.1 (Table 1; Fig. 4). $T_{h(v)}$ was between 220 and 250 °C, somewhat higher than the range of $T_{h(v)}$ values (70 to 200 °C) reported by Gillen et al. (2004*a*) for quartz from Wernecke Breccia matrix in the Igor area but similar to the upper range of homogenization temperatures (80 to 300 °C) for inclusions in dolomite, calcite, fluorite, and quartz in magnetite-rich assemblages reported by Hitzman et al. (1992).

Olympic area: Zoned quartz from the matrix of Wernecke Breccia in the Olympic area contains small clusters of fluid inclusions that are interpreted to be primary (i.e., syn-breccia). At room temperature, the inclusions contain liquid (~80%) plus vapor (~20%). Phase changes were difficult to observe because of the small size of inclusions. Initial melting temperatures varied from –67 to –60 °C, and $T_{m(ice)}$ ranged from –29 to –26 °C; salinity is ~26 to 28 wt.% NaCl equiv. (Table 1). Homogenization occurred by vapor bubble disappearance between 158 and 170 °C (Table 1; Fig. 4).

Summary of fluid inclusion results

Fluid inclusion data presented here indicate that breccia-forming fluids in the Slab area were highly saline (~42 wt.% NaCl equiv.), whereas those at the remaining prospects had moderate salinity (24–38 wt.% NaCl equiv.). Fluids at Slab were Na-dominant, those at Hoover and Slats-Frosty varied from Na- to Ca-dominant, and those at Igor were at least, in part, Ca-dominant. Syn-breccia fluid in the Slab area had minimum temperatures of 226 to 245 °C. Minimum fluid temperatures at the other prospects were lower than those at Slab and ranged from 112 to 188 °C, with the exception of Igor (see later in the text).

Fluid inclusion data from this study are clearly not abundant, but the results do agree in general with the limited data that has been published for the Wernecke Breccias. Hitzman et al. (1992) reported homogenization temperatures of 80 to 300 °C and salinities of 5 to 15 wt.% NaCl equiv. for fluid inclusions in dolomite, calcite, fluorite, and quartz from the Igor prospect (Fig. 4). Gillen et al. (2004*a*) measured homogenization temperatures of 70 to 200 °C for fluid inclusions in quartz from the Hoover and Igor prospects. Kendrick et al. (2008) examined samples from all six prospects and reported homogenization temperatures of 100 to 250 °C for L + V inclusions and 175 to 290 °C for L + V + daughter inclusions, together with salinities of 10 to 44 wt.% NaCl equiv. (Fig. 4).

Stable isotopes

Mineral separates from Wernecke Breccia and associated veins were analyzed for carbon and oxygen (n = 94), sulfur (n = 49), and hydrogen (n = 14) isotopes. Samples were chosen from various paragenetic stages at each prospect to document changes in the fluids that may have occurred through time and to compare fluids from prospects hosted in different parts of the Wernecke Supergroup. In addition, 23 samples of limestone/dolostone and three samples of carbonaceous shale were analyzed for carbon and oxygen isotopes to characterize regional host rocks. Results are summarized in Tables 2 to 5 and presented in Figs. 5, 6, 7; complete results are in Hunt (2005).

Methods

Carbon and oxygen isotopes

Carbonates were extracted by crushing and hand picking under a binocular microscope and identified using X-ray diffraction (GADDS, general area detector diffraction system) at the James Cook University Advanced Analytical Centre. Whole-rock samples were crushed and powdered. Isotopic analyses of mineral separates and whole-rock samples were carried out at the University of Tasmania Central Science Laboratory using a modification of the method of McCrea (1950). Samples were reacted with H_3PO_4 at 50 °C for a 24 hour period, followed by extraction of CO_2 in a chemical

Table 1. Summary of syn-breccia fluid inclusion data for samples from IOCG prospects in the Wernecke Mountains area.

Prospect	FI paragenesis	*n*	FI type	$T_{m(ice)}$ (°C)	$T_{m(hh)}$ (°C)	$T_{h(v)}$ (°C)	$T_{h(s)}$ (°C)	T_h (°C)	NaCl equiv. (wt.%)	Na:Ca (wt.%)
Slab	Primary	10	L+V+H	–50 to –36	na	154 – 175	226 – 245	226 – 245	41 – 42	1.3 – 1.4
Hoover	Secondary	7	L+V	–34 to –25	na	153 – 172	na	153 – 172	26 – 32	0.4, 0.7
Hoover	Secondary	1	L+V+H	–30	na	165	188	188	38	1.20
Slats-F	Pseudo secondary	6	L+V	–28 to –23	–12, –8	112 – 160	na	112 – 160	24 – 28	0.8 – 1.1
Slats-F	Pseudo secondary	6	L+V+H	–28 to –23	–4 to 3	89 – 160	>160	>160	24 – 29	1.0 – 1.6
Slats-F	Pseudo secondary	4	L+V+Op	–35 to –26	–22 to 0	68 – 130	>130	>130	27 – 32	1.0 – 1.6
Slats-F	Pseudo secondary	1	L+V+H+Op	–28	–7	124	>124	>124	29	0.9
Igor	Primary	3	L+V	–54 to –50	–26	220 – 250	na	220 – 250	~34	~0.1
Olympic	Primary	7	L+V	–29 to –26	na	158 – 170	na	158 – 170	26 – 28	na

Note: $T_{m(ice)}$, ice-melting temperature; $T_{m(hh)}$, hydrohalite melting temperature; $T_{h(v)}$, vapor homogenization temperature; $T_{h(s)}$, halite dissolution temperature; T_h, final homogenization temperature; *n*, number of samples. NaCl equiv. wt.% values for Slab were approximated using graphical methods of Vanko et al. (1988) and Zwart & Touret (1994). Values for other areas were calculated from $T_{m(ice)}$, $T_{m(hh)}$, $T_{h(s)}$ using the programme FlinCalc (J. Cleverley, written communication, 2003), which uses information from Zhang and Frantz (1987) and Brown (1998). FI, fluid inclusion; L, liquid; V, vapor; H, halite; Op, opaque. wt.% NaCl equiv. includes $CaCl_2$ wt.%; Na:Ca = (wt.% NaCl/wt.% $CaCl_2$)/(molecular weight NaCl/molecular weight $CaCl_2$); na, not available.

separation line. Gas was analyzed on a Micromass Optima Stable Isotope mass spectrometer. Results were corrected for machine error and are expressed relative to V-SMOW and PDB. Previous analyses of the Biggenden calcite, used as the international standard, have a standard error of ± 0.06‰ for $\delta^{13}C$ and ± 0.1‰ for $\delta^{18}O$ (at 1σ).

Sulfur isotopes: Sulfides and sulfates were extracted by crushing and hand picking under a binocular microscope after the preparation of cut slabs and petrographic inspection of the sulfide and sulfate phases for contaminant inclusions. Isotopic analyses were carried out at the University of Tasmania Central Science Laboratory, Hobart, Australia, using the method of Robinson and Kusakabe (1975). Powdered samples were reacted with cuprous oxide at high temperatures, SO_2 was then separated from H_2O, CO_2 and noncondensable gases in a chemical separation line. Gas was analyzed on a Sira VG Series 2 mass spectrometer. Results were corrected for machine error and are expressed relative to Cañon Diablo Troilite (CDT). Results were calibrated against a secondary gas standard and were reproducible to within 0.2‰.

Hydrogen and oxygen isotopes

Muscovite, biotite, and actinolite were extracted by crushing and hand picking under a binocular microscope after petrographic and microprobe analysis of the phases. Fourteen mineral separates from three of the prospects (Slab, Hoover, and Igor) were selected for hydrogen and oxygen isotope analysis. Unfortunately, the other study areas did not yield suitable material for analysis. Analyses were carried out at the Scottish Universities Environmental Research Centre, East Kilbride, Scotland. Oxygen was extracted using a laser fluorination system based on that of Sharp (1990), converted to CO_2, and analyzed on a VG PRISM III mass spectrometer, with analytical precision of ± 0.1‰ (at 1σ). Hydrogen was extracted by the method described in Fallick et al. (1993), except that hot chromium rather than uranium was used (see Donnelly et al. 2001). Reproducibility of isotopically homogeneous material was ± 5‰ (at 1σ), and NBS 30 gave a δD value of –65‰. All data are reported relative to V-SMOW.

No indications of alteration were found during petrographic and microprobe analyses of the samples. However, two biotite samples gave abnormally high yields of hydrogen and may have been chloritized (Table 5). In addition, three samples of muscovite failed to generate sufficient hydrogen for analysis. These five samples have been omitted from the following discussion.

Results of carbon and oxygen isotopic analyses

Wernecke Supergroup

Calcite from limestone layers in the Fairchild Lake Group has $\delta^{18}O$ and $\delta^{13}C$ values of 11.8‰ to 14.4‰ and –2.0‰ to 0.4‰, respectively (Table 2, Fig. 5). Ankerite and ferroan dolomite from a dolostone layer in the Quartet Group has $\delta^{18}O$ and $\delta^{13}C$ values similar to those of the Fairchild Lake Group (13.9‰ to 15.9‰ and –1.9‰ to –0.3‰, respectively). Dolomite from dolostone layers, stromatolitic dolostone, and intraformational breccia within the Gillespie Lake Group has $\delta^{18}O$ values (16.4‰ to 24.6‰) significantly heavier than those of the Fairchild Lake Group and Quartet Group

Fig. 4. Summary of fluid inclusion data for samples from the Wernecke Mountains. T_h, final homogenization temperature; NaCl eq. wt.%, equivalent weight percent NaCl. See text for details of salinity calculations. Black bars, data from this study; grey bars, data from Gillen et al. (2004a); 1 and 2, from Hitzman et al. (1992); 3, from Gillen et al. (2004a); 4 and 5, from Kendrick et al. (2008).

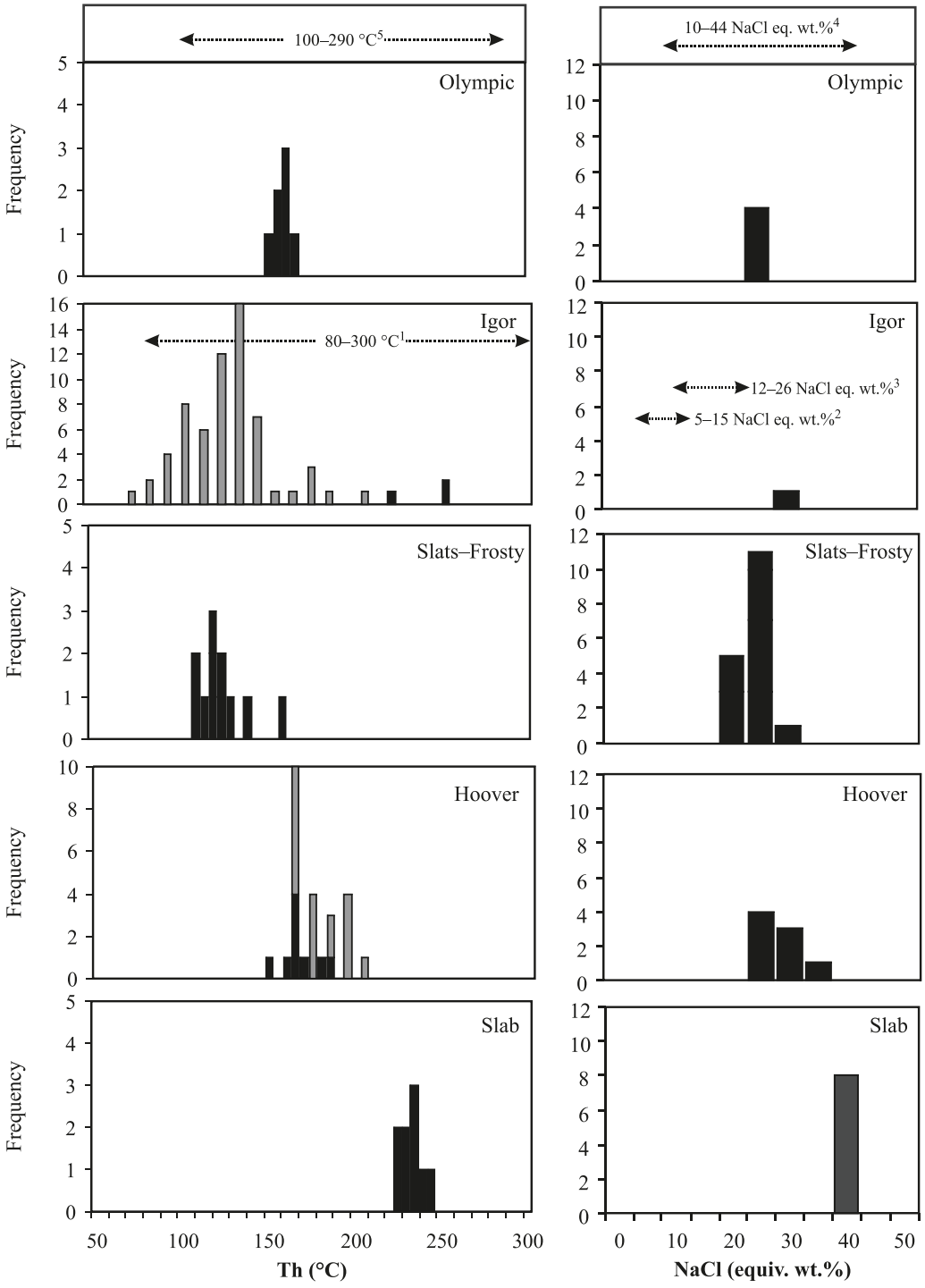

but similar $\delta^{13}C$ values (–1.9‰ to 1.6‰). Whole-rock samples of Quartet Group carbonaceous shale have $\delta^{13}C$ values of –26.7‰ to –20.8‰.

Slab area

Samples of ankerite–magnetite alteration, veins, and breccia that formed early in the brecciation at Slab have $\delta^{18}O$ and $\delta^{13}C$ values of 10.9‰ to 14.8‰ and –3.7‰ to –1.2‰, respectively (Table 2; Fig. 5*a*). Samples from the main brecciation phase have $\delta^{18}O$ values between –2.1‰ and 15.3‰ and $\delta^{13}C$ values of –3.7‰ to 1.5‰. Results for samples collected from veins that crosscut breccia partially overlap those of the earlier stage, with $\delta^{18}O$ and $\delta^{13}C$ values from 10.1‰ to 14.6‰ and –2.7‰ to 1.2‰, respectively.

Locally, coexisting hydrothermal calcite and dolomite have $\delta^{18}O$ values of 13.0‰ and 14.1‰, respectively. The differ-

Table 2. Summary of carbon and oxygen isotope results for carbonate samples from IOCG prospects in the Wernecke Mountains area plus Wernecke Supergroup limestone, dolostone, and carbonaceous shale.

Sample	*n*	$\delta^{13}C$ (‰ PDB)	$\delta^{18}O$ (‰ SMOW)
All WSG limestone & dolostone	23	–2.0 to 1.6	11.8 to 24.6
Fairchild Lake Group	6	–2.0 to 0.4	11.8 to 14.4
Quartet Group carbonate	3	–1.9 to –0.3	13.9 to 15.9
Quartet Group carbonaceous shale	4	–26.7 to –20.8	N/A
Gillespie Lake Group	14	–1.9 to 1.6	16.4 to 24. 6
*Mean value for ca. 1.8–1.7 Ba carbonates		–2 to 2	18 to 22
All breccia-related carbonates	94	–10.6 to 1.5	–2.1 to 20.0
Slab (pre- to syn-breccia)	11	–3.7 to –1.2	10.9 to 14.8
Slab (syn-breccia)	13	–3.7 to 1.5	–2.1 to 15.3
Slab (syn- to post-breccia)	6	–2.7 to 1.2	10.1 to 14.6
Hoover (syn-breccia)	8	–6.8 to –2.3	9.4 to 13.5
Slats W (syn- & syn- to post-breccia)	11	–10.6 to –2.2	14.1 to 16.8
Slats F (pre-, syn-, & syn- to post-breccia)	9	–4.4 to –0.2	13.7 to 20.1
Igor (syn- & syn- to post-breccia)	14	–6.1 to –1.4	14.6 to 20.0
Olympic (syn-, syn- to post-, & post-breccia)	19	–5.1 to 0.4	14.8 to 18.7

Note: WSG, Wernecke Supergroup; n, number of samples; PDB, Pee Dee belemnite; SMOW, standard mean ocean water; N/A, not available. *Mean value for ca. 1.8 to 1.7 Ba carbonates is from Shields and Veizer (2002).

Table 3. $\delta^{18}O_{water}$ values calculated from measured $\delta^{18}O$ values of syn-breccia carbonate samples from IOCG prospects in the Wernecke Mountains area.

Prospect	Measured $\delta^{18}O_{carbonate}$ (‰ SMOW)	Calculated $\delta^{18}O_{water}$ (‰ SMOW)	Temperature used in calculation (°C)
Slab	–2.1 to 15.3	–7.9 to 9.5	300
Hoover	9.4 to 13.5	3.0 to 7.2	285
Slats-Frosty	13.7 to 20.1	5.4 to 11.6	235
Igor	14.6 to 20.0	9.4 to 14.7	355
Olympic	16.6 to 18.7	5.7 to 7.8	185

Table 4. Summary of sulfur isotope results for sulfides and sulfates in samples from IOCG prospects in the Wernecke Mountains area.

Sample	*n*	$\delta^{34}S$ (‰ CDT)
All breccia-related samples	49	–12.4 to 17.1
Slab	20	–11.5 to 7.1
Hoover	8	–12.4 to 13.4
Slats Wallbanger	4	–6.8 to –1.7
Slats Frosty	1	4.2
Igor (sulfides)	8	–8.4 to 4.8
Igor (barite)	5	7.7 to 17.1
Olympic	3	–10.8 to 5.3

Note: *n*, number of samples; CDT, Cañon Diablo Troilite.

ence in $\delta^{18}O$ values between the two types of carbonate indicates a fluid temperature of ~300 °C, based on the fractionation factors of Sheppard and Schwarcz (1970) or Golyshev et al. (1981) as reported in Beaudoin and Therrien (2008).

Hoover area

Syn-breccia calcite from the Hoover prospect has $\delta^{18}O$ and $\delta^{13}C$ values of 9.4‰ to 13.5‰ and –6.8‰ to –2.3‰, respectively (Table 2). The lowest $\delta^{13}C$ values were found in samples from veins and breccia that cut Quartet Group carbonaceous slate/shale; higher values were found in samples from veins and breccia cutting calcareous metasiltstone (Fig. 5*b*).

Slats-Frosty area

Samples of syn- and syn- to post-breccia carbonate from the Slats-Frosty area have a fairly narrow range of $\delta^{18}O$ values between 13.7‰ and 20.1‰, with most samples falling between 13.7‰ and 15.6‰ (Fig. 5*c*; Table 2). $\delta^{13}C$ values range from –4.4‰ to –0.2‰, with the lowest values in veins that crosscut carbonaceous shale.

Slats-Wallbanger area

Syn- and syn- to post-breccia carbonate from the Slats-Wallbanger area have a narrow range of $\delta^{18}O$ values (14.1‰ to 16.8‰) and a wide range of $\delta^{13}C$ values (–10.6‰ to –2.2‰; Table 2; Fig. 5*d*). All but two $\delta^{13}C$ values are <–4‰. The highest $\delta^{13}C$ values were found in veins cutting interlayered metasiltstone and dolostone at the base of Gillespie Lake Group, and the lowest values were found in veins that cut a massive magnetite ± ankerite vein.

Igor area

Syn- and syn- to post-breccia siderite and ferroan dolomite from the Igor prospect have $\delta^{18}O$ values of 14.6‰ to 20.0‰ and $\delta^{13}C$ values of –6.1‰ to –1.4‰ (Table 2; Fig. 5*e*).

Olympic area

Syn-breccia, syn- to post-breccia, and post-breccia carbonate from the Olympic area have returned a fairly narrow range of oxygen and carbon isotope values with $\delta^{18}O$ between 14.8‰ to 18.7‰ and $\delta^{13}C$ from –5.1‰ to 0.4‰ (Table 2; Fig. 5*f*). Locally, coexisting dolomite and ankerite have $\delta^{18}O$ values of 14.8‰ and 15.6‰, respectively.

Table 5. Summary of hydrogen and oxygen isotope results for samples from IOCG prospects in the Wernecke Mountains area.

Area	Mineral	Mode	Paragenesis	δD (‰ V-SMOW)	$\delta^{18}O$ (‰ V-SMOW)	δD_{water} (‰ V-SMOW)	$\delta^{18}O_{water}$ (‰ V-SMOW)
Slab	Muscovite	V	SB	–21	11.6	27.2	8.1
Slab	Muscovite	BM	SB or STPB	–45	10.6	3.2	8.2
Slab	Muscovite	V	SB	–54	11.1	–5.8	9.6
Igor	Muscovite	BM	STPB	–55	9.9	–6.8	7.5
Slab	Biotite	V	SB	–141	6.7	–73.4	7.8
Slab	Biotite	BM	SB	–115	8.3	–47.4	9.4
Slab	Biotite	BM	SB	–84	9.5	–16.4	10.6
Hoover	Biotite	V	SB or STPB	–119	7.8	–38.4	8.1
Slab	Actinolite	V	STPB	–22	11.0	–0.3	11.0
Slab#	Actinolite	V	STPB	–18	11.0	3.7	11.0
Not used in figures							
Hoover	Muscovite	V	SB	no data	11.1	no data	9.3
Slab	Muscovite	V	SB	no data	11.5	no data	10.1
Slab	Muscovite	BM	STPB	no data	10.1	no data	8.7
Slab	Biotite*	V	STPB	–23	8.1	44.6	9.2
Slab	Biotite*	BM	SB	–34	8.7	33.6	9.8

Note: Also shown are calculated δD_{water} and $\delta^{18}O_{water}$ values for co-existing water. See Fig. 7 caption for calculation details. V-SMOW, Vienna standard mean ocean water; V, vein; BM, breccia matrix; SB, syn-breccia; STPB, syn- to post-breccia; #, duplicate analysis; *, possible chloritization of biotite.

Summary and discussion of carbon and oxygen isotope results

The low $\delta^{13}C$ values of samples of Quartet Group carbonaceous shale are consistent with an organic matter source for the carbon. Mean $\delta^{18}O$ and $\delta^{13}C$ values for Paleoproterozoic carbonates comparable in age to the Wernecke Supergroup are 18‰ to 22‰ and –2‰ to 2‰, respectively (e.g., Shields and Veizer 2002). Samples from Wernecke Supergroup limestone and dolostone have $\delta^{13}C$ values similar to the mean values but variable $\delta^{18}O$ values (Fig. 5). $\delta^{18}O$ values similar to the mean $\delta^{18}O$ values were found in samples from the Gillespie Lake Group (~16‰–25‰, Table 2), which forms the upper part of Wernecke Supergroup. However, samples from the lower and middle parts of the Wernecke Supergroup (i.e., the Fairchild Lake and Quartet groups) have $\delta^{18}O$ values lower than the mean values (~12‰–16‰). Thus, although the number of samples collected from the Wernecke Supergroup is not large, the results suggest that the lower and middle parts of the supergroup are significantly depleted in ^{18}O compared with typical Proterozoic marine carbonate. The Wernecke Supergroup samples were collected from areas outside those with visible Wernecke Breccia-related alteration assemblages; therefore, this variation may reflect a meteoric water-dominated diagenetic history for pre-Gillespie Lake Group strata or post-Wernecke Supergroup carbonate alteration that preferentially affected the lower and middle Wernecke Supergroup. However, Wernecke Breccia bodies cover a wide geographic area and have extensive alteration haloes, so the possibility of changes to the isotopic compositions of Wernecke Supergroup carbonates because of breccia-related alteration cannot be ruled out.

In general, carbon and oxygen isotope values for the prospects studied do not vary systematically with paragenetic stage. An exception to this is the Slab prospect, where early ankerite–magnetite alteration forms a distinct group with $\delta^{18}O$ values of 10.9‰ to 14.8‰ and $\delta^{13}C$ values of –3.7‰ to –1.2‰ (Fig. 5*a*; Table 2).

Some of the spread in $\delta^{18}O$ values in samples from the prospects and the Wernecke Supergroup may be because of the expected fractionation of oxygen isotopes between different types of carbonate (e.g., Rye and Ohmoto 1974; Valley et al. 1986; Zheng 1999). For example, dolomite ($\delta^{18}O$ = 14.8‰) and ankerite ($\delta^{18}O$ = 15.6‰) from the Olympic prospect indicate $\Delta_{dolomite–ankerite}$ = 0.8, which is close to the expected value of 0.97 (@ 185 °C — average trapping temperature from fluid inclusions) calculated using the fractionation factors of Zheng (1999), suggesting it may be owing to equilibrium isotopic fractionation.

Measured oxygen isotope ratios of syn-breccia carbonates were used in conjunction with the fractionation factors of Zheng (1999) for calcite-H_2O, dolomite-H_2O, ankerite-H_2O and siderite-H_2O along with estimates of temperature (as shown in Table 7) for syn-breccia fluid to calculate $\delta^{18}O_{water}$ values for the prospects. $\delta^{18}O_{water}$ values range from –7.9‰ to 9.5‰ for samples from the Slab area, 3.0‰ to 7.2‰ for samples from the Hoover area, 5.4‰ to 11.6‰ for samples from the Slats-Frosty area, 9.4‰ to 14.7‰ for samples from the Igor area, and 5.7‰ to 7.8‰ for samples from the Olympic area (Table 3; shown for comparison on Fig. 7).

Results of sulfur isotopic analyses

Slab area

Pre- to syn-breccia, syn-breccia, and syn- to post-breccia sulfide (pyrite, chalcopyrite) samples from the Slab area have overlapping $\delta^{34}S$ values between –11.5‰ and 7.1‰ (Table 4; Fig. 6*a*). Samples from the same paragenetic stage show a wide range of values. For example, two samples of chalcopyrite from a syn-breccia vein have $\delta^{34}S$ values of –11.5‰ and 2.4‰ (labeled 1 in Fig. 6*a*); samples of chalcopyrite from syn- to post-breccia veins have values of $\delta^{34}S$ = –11.0‰ and 3.8‰ (labeled 2 in Fig. 6*a*).

Hoover area

Syn-breccia and syn- to post-breccia sulfide (pyrite, chalcopyrite) samples from the Hoover prospect have a wide

Fig. 5. Results of oxygen and carbon isotopic analyses for samples from the (*a*) Slab, (*b*) Hoover, (*c*) Slats-Frosty (Slats-F), (*d*) Slats-Wallbanger (Slats-W), (*e*) Igor, and (*f*) Olympic areas. Also shown are results for host Wernecke Supergroup samples of Fairchild Lake Group (FLG), Quartet Group (QG), and Gillespie Lake Group (GLG). (*g*) Overall $\delta^{18}O$ versus $\delta^{13}C$ results for carbonate samples from the Wernecke Mountains. Also shown are fields for common large earth reservoirs that are important in hydrothermal systems. Fields are from Rollinson (1993). Legend is in (*a*). V-PDB, Vienna Pee Dee belemnite; V-SMOW, Vienna standard mean ocean water.

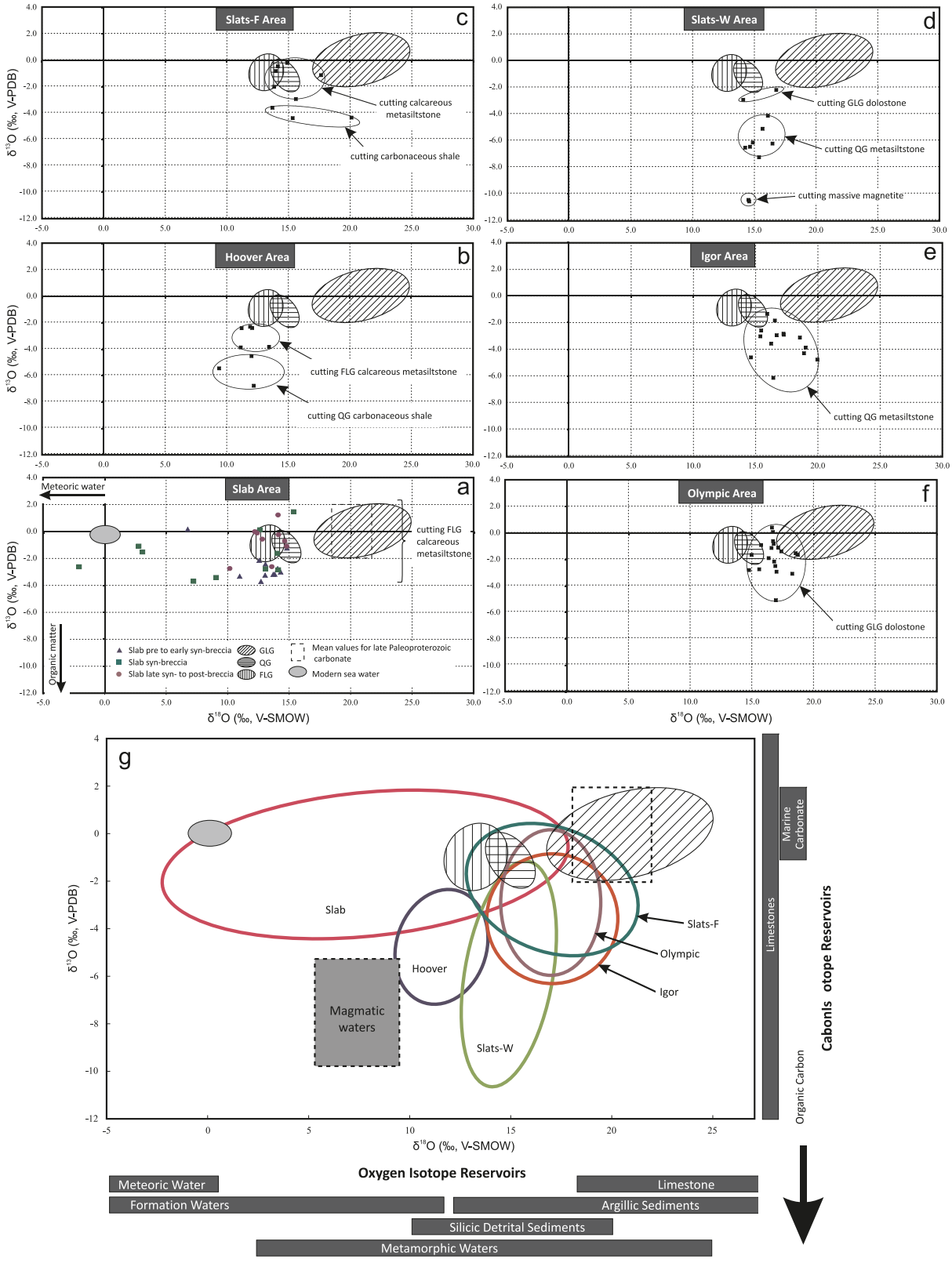

Fig. 6. Results of sulfur isotope analyses for samples from the (*a*) Slab, (*b*) Hoover, (*c*) Slats, (*d*) Igor, and (*e*) Olympic areas. Also shown are fields for common large earth reservoirs that are important in hydrothermal systems. Fields are from Rollinson (1993). See text for explanation of the numbers shown in some bars. CDT, Cañon Diablo Troilite; FLG, Fairchild Lake Group; QG, Quartet Group.

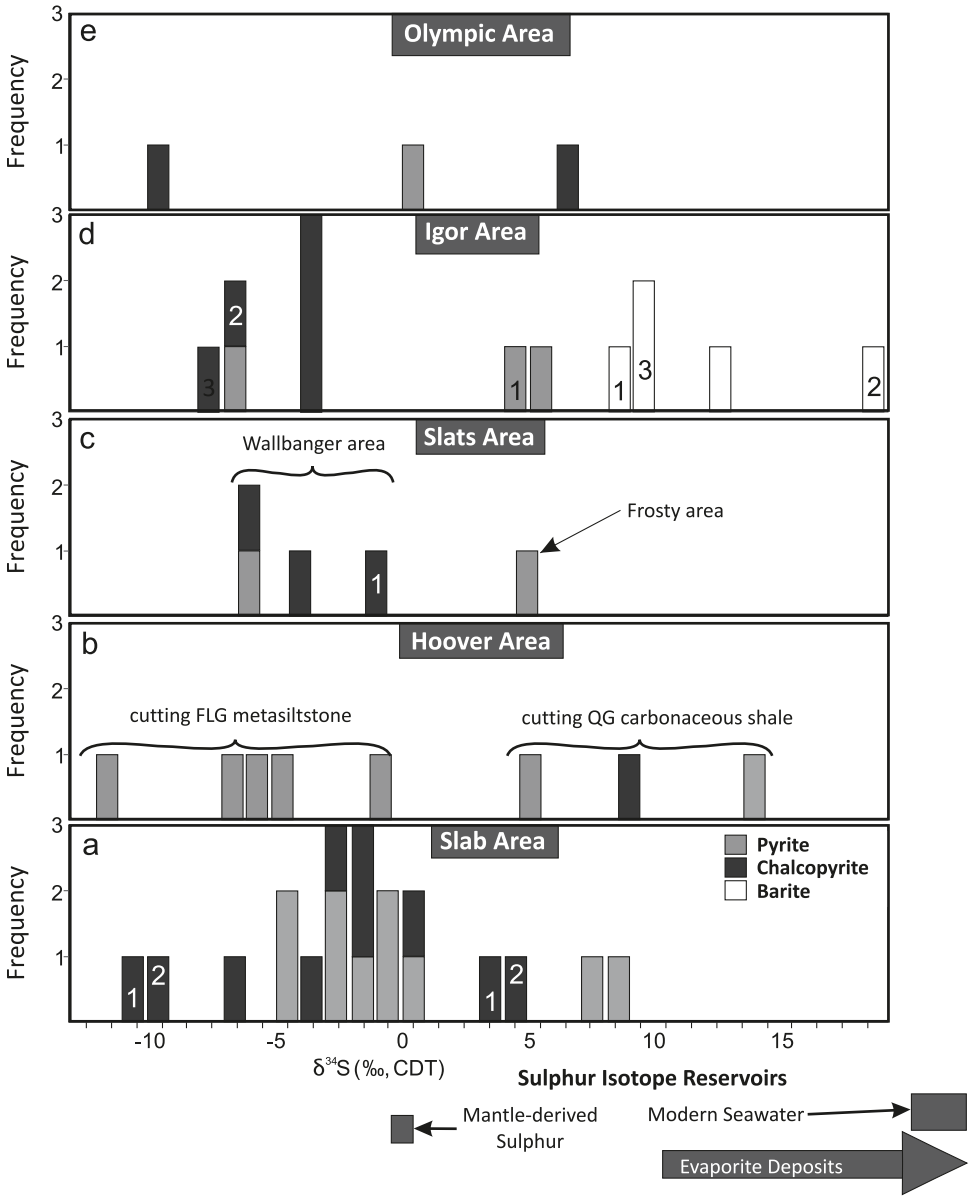

range of $\delta^{34}S$ values between –12.4‰ and 13.4‰ with no systematic variation with paragenetic stage (Table 4; Fig. 6*b*), although, based on the limited data, there is variation in $\delta^{34}S$ with host rock type. Samples from veins and breccia hosted in calcareous metasiltstone have $\delta^{34}S$ values of –12.4‰ to –1.6‰, whereas samples from those hosted in carbonaceous shale/slate have $\delta^{34}S$ value of 4.6‰ to 13.4‰ (Fig. 6*b*).

Slats area

Syn-breccia and syn- to post-breccia sulfides (pyrite, chalcopyrite) from the Slats-Wallbanger area have $\delta^{34}S$ values between –6.8‰ and –1.7‰ (Table 4; Fig. 6*c*). The highest $\delta^{34}S$ value (–1.7‰) is from a syn- to post-breccia ankerite–chalcopyrite–quartz vein that cuts massive magnetite (labeled 1 in Fig. 6*c*). The remaining values are from syn-breccia veins that cut calcareous siltstone at the base of Gillespie Lake Group. Pyrite from a hematite–pyrite–quartz vein (paragenetic stage unknown) cutting Fairchild Lake Group phyllite at Slats-Frosty has a $\delta^{34}S$ value of 4.2‰ (Fig. 6*c*).

Igor area

Syn-breccia and syn- to post-breccia sulfides (pyrite, chalcopyrite) from the Igor prospect have $\delta^{34}S$ values between –8.4‰ and 4.8‰ (Table 4; Fig. 6*d*). Igor is the only prospect in the study that contains significant amounts of sulfate, as syn- to post-breccia barite. Samples of the barite have $\delta^{34}S$ values between 7.7‰ and 17.1‰. Samples of co-existing sulfate and sulfide were analyzed and gave the following results: (1) pyrite from the selvage of a barite vein had a $\delta^{34}S$ value of 3.3‰ and $\delta^{34}S_{barite}$ value of 7.7‰ (labeled 1 in Fig. 6*d*), (2) chalcopyrite and barite from a hematite–magnetite–chalcopyrite–barite vein had $\delta^{34}S$ values of –7.9‰ and 17.1‰, respectively (labeled

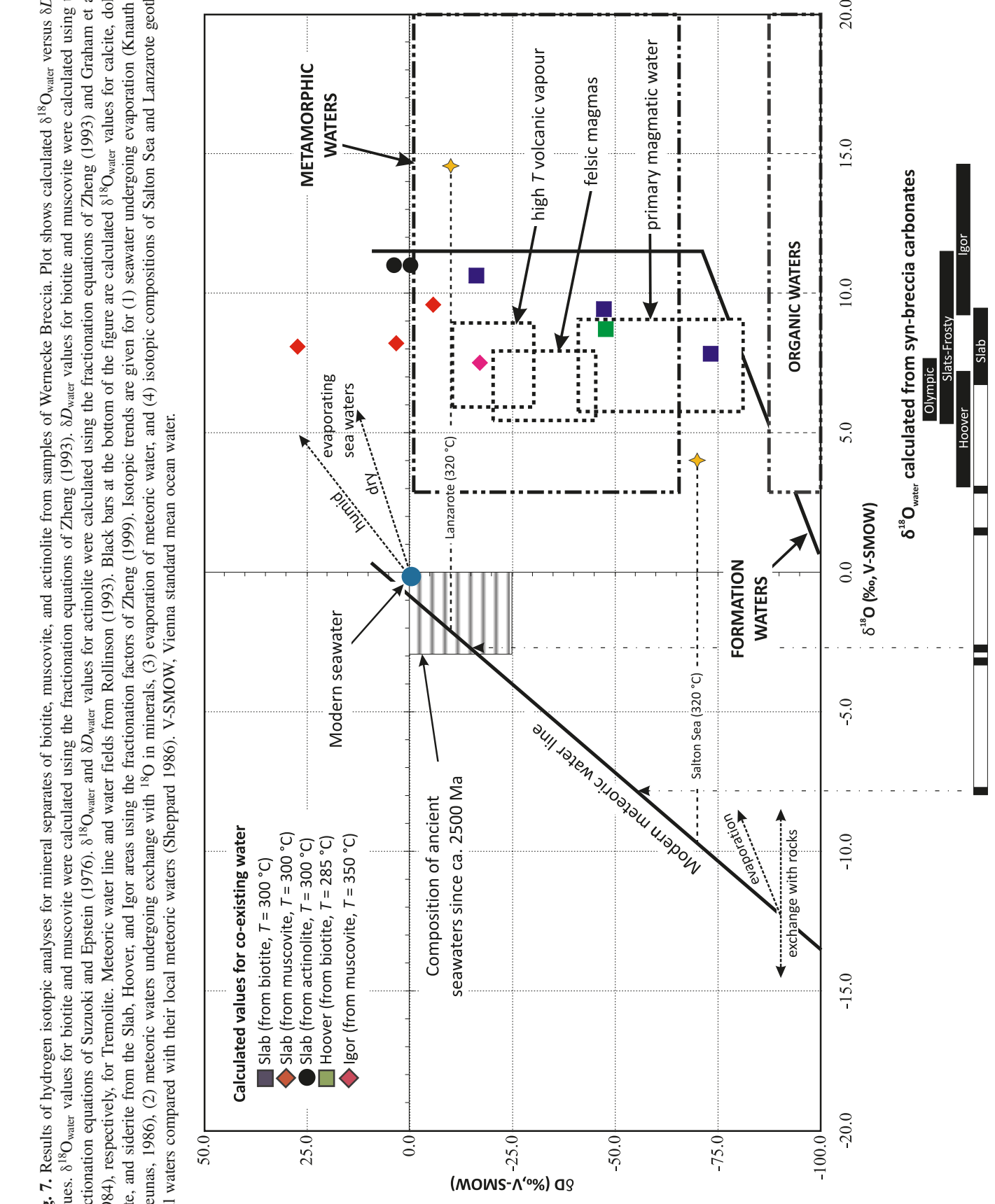

Fig. 7. Results of hydrogen isotopic analyses for mineral separates of biotite, muscovite, and actinolite from samples of Wernecke Breccia. Plot shows calculated $\delta^{18}O_{water}$ versus δD_{water} values. $\delta^{18}O_{water}$ values for biotite and muscovite were calculated using the fractionation equations of Zheng (1993). δD_{water} values for biotite and muscovite were calculated using the fractionation equations of Suzuoki and Epstein (1976). $\delta^{18}O_{water}$ and δD_{water} values for actinolite were calculated using the fractionation equations of Zheng (1993) and Graham et al. (1984), respectively, for Tremolite. Meteoric water line and water fields from Rollinson (1993). Black bars at the bottom of the figure are calculated $\delta^{18}O_{water}$ values for calcite, dolomite, and siderite from the Slab, Hoover, and Igor areas using the fractionation factors of Zheng (1999). Isotopic trends are given for (1) seawater undergoing evaporation (Knauth and Beeunas, 1986), (2) meteoric waters undergoing exchange with ^{18}O in minerals, (3) evaporation of meteoric water, and (4) isotopic compositions of Salton Sea and Lanzarote geothermal waters compared with their local meteoric waters (Sheppard 1986). V-SMOW, Vienna standard mean ocean water.

2 in Fig. 6*d*), and (3) chalcopyrite and barite from a siderite–chalcopyrite–pyrite–barite vein had $\delta^{34}S$ values of –8.4‰ and 8.7‰, respectively (labeled 3 in Fig. 6*d*). Samples 2 and 3 give reasonable temperatures of 243 and 356 °C based on the equations of Ohmoto and Lasaga (1982: 1000 lnα sulphate-pyrite = $6.463 \times 10^6/T^2 + 0.56$; 1000 ln$\alpha$ sulphate-chalcopyrite = $6.513 \times 10^6/T^2 + 0.56$, where T is temperature in Kelvin). Sample 1 gives a temperature of 1026 °C, which indicates this barite–pyrite pair were not in equilibrium (e.g., Ohmoto and Goldhaber 1997).

Olympic area

Abundant sulfides were not observed in the Olympic area and only three samples were analyzed. Syn-breccia and syn- to post-breccia chalcopyrite have $\delta^{34}S$ values of –10.8‰ and 5.3‰, respectively (Table 4; Fig. 6*e*). Pyrite in Wernecke Breccia proximal to diorite has a $\delta^{34}S$ value of –0.5‰.

Summary and discussion of sulfur isotope results

Sulfide samples from the Wernecke Mountains have a wide range of $\delta^{34}S$ values from approximately –12‰ to 13‰ with most values between –7‰ and 0‰. In general, the isotopic ratios do not vary systematically with paragenetic stage and can vary greatly even within a single stage. This is illustrated in the Slab area, where chalcopyrite samples collected a few centimetres apart in a vein have $\delta^{34}S$ values of –11.5‰ and +2.4‰. This variability may be explained by (1) changes in the temperature of the fluid, (2) changes in the oxidation state of the fluid, (3) variations in the SO_4^{-2}/H_2S ratio, and (4) different sources of sulfur (e.g., Ohmoto and Rye 1979; Ohmoto and Goldhaber 1997). If the dominant species in a hydrothermal fluid is H_2S, temperature variations cause little change in $\delta^{34}S$ of sulfide minerals (Ohmoto and Goldhaber 1997). However, if the fluid contains significant amounts of SO_4^{-2} and H_2S (or other oxidized and reduced species) a change in temperature can cause large variations in the $\delta^{34}S$ values of minerals precipitating from the fluid (Ohmoto and Goldhaber 1997). In open systems, the ratio of oxidized to reduced sulfur species can be changed by reactions with wall rocks (e.g., by reaction with Fe^{+2}- or Fe^{+3}-bearing minerals, such as magnetite and hematite) or by precipitation of sulfide or sulfate minerals (Ohmoto and Goldhaber 1997). Oxidation of the fluid (i.e., an increase in the ratio of oxidized to reduced species) will cause a decrease in the $\delta^{34}S$ values of individual species in the fluid under equilibrium conditions and reduction may cause an increase (Ohmoto and Goldhaber 1997). Reduction of fluid can also occur by reaction with organic matter, causing an increase in the $\delta^{34}S$ values of H_2S and SO_4^{-2} and of minerals precipitated from this fluid (Ohmoto and Goldhaber 1997). Indications of this are seen at the Hoover prospect, where veins and breccia hosted in carbonaceous shale have higher $\delta^{34}S$ values than those hosted in calcareous metasiltstone (Fig. 6*b*).

At Igor, one barite sample has a $\delta^{34}S$ value (17.1‰) similar to that of Proterozoic seawater (18‰, Strauss 1993), suggesting possible derivation of sulfur from the seawater. In the Hoover area, some sulfur may have been leached from biogenic pyrite associated with organic matter because sulfide hosted in carbonaceous shale has different $\delta^{34}S$ values than sulfide hosted in metasiltstone (Fig. 6*b*). At Olympic, a sample of pyrite from Wernecke Breccia that is adjacent to Bonnet Plume River Intrusions diorite has a $\delta^{34}S$ value of 0‰, suggesting some sulfur may have been derived locally from igneous rocks.

Results of hydrogen isotope analyses

Biotite from Wernecke Breccia matrix in the Slab area has δD values of –115‰ and –84‰ and $\delta^{18}O$ values of 8.3‰ and 9.5‰ (Table 5). A sample of muscovite from breccia matrix has a δD value of –45‰ and a $\delta^{18}O$ value of 10.6‰. Biotite from a vein in a breccia clast in the Slab area has δD and $\delta^{18}O$ values of –141‰ and 6.7‰, respectively. Muscovite in veins cutting altered Fairchild Lake Group proximal to Wernecke Breccia in the Slab area has δD values of –54‰ and –21‰ and $\delta^{18}O$ values of 11.1‰ and 11.6‰; actinolite from a vein in this area has δD values of –22‰ and –18‰ and a $\delta^{18}O$ value of 11.0‰. A sample of biotite from Wernecke Breccia matrix at the Hoover prospect has δD and $\delta^{18}O$ values of –119‰ and 7.8‰, respectively (Table 5). A sample of muscovite from Wernecke Breccia matrix in the Igor area has δD and $\delta^{18}O$ values of –55‰ and 9.9‰, respectively (Table 5).

Deuterium and oxygen isotope values for water co-existing with syn-breccia muscovite, biotite, and actinolite were calculated using the measured hydrogen and oxygen isotopic ratios; fractionation factors for muscovite–H_2O, biotite–H_2O, and actinolite–H_2O (or tremolite–H_2O); and estimates of temperature from the fluid inclusion analyses. Calculated $\delta^{18}O_{water}$ values for the three prospects fall within a fairly narrow range from 7.8‰ to 11‰ (Table 5; Fig. 7). However, there is a wide spread in calculated δD_{water} values; those calculated from biotite and muscovite range from –73.4‰ to –16.4‰ and –6.8‰ to +27.2‰, respectively. δD_{water} values calculated from actinolite are –0.3‰ and 3.7‰.

Low and (or) variable δD values in the Wernecke samples could be because of (1) mixing of different waters, (2) evaporation, (3) interaction with younger fluids, (4) exchange with hydrous minerals, (5) fractionation during membrane filtration, and (6) exchange with H_2S (e.g., Sheppard 1986; Ohmoto 1986). However mixing and evaporation are considered to be most likely. For example, organic water derived from carbonaceous material in host Wernecke Supergroup rocks would have low δD values and could be present in variable amounts in the fluid. Evolved meteoric water (or seawater) formed by evaporation, with consequent higher δD values (Fig. 7; e.g., Sheppard 1986), could also be present in the breccia-forming fluids because arid conditions are indicated at least during the deposition of the lower part of the Wernecke Supergroup by the presence of evaporites in the Fairchild Lake Group (Hunt et al. 2005). However, it should be noted that muscovite in Wernecke Breccia and associated veins demonstrates Ar–Ar re-equilibration (Hunt 2005), most likely because of re-heating, and it is not clear what effect, if any, this would have had on the hydrogen isotopic ratios.

The $\delta^{18}O$ values calculated for water co-existing with biotite, muscovite, and actinolite in samples of Wernecke Breccia are similar to those calculated for water co-existing with carbonate at the six prospects (Fig. 7). This could be because of their precipitation from fluid with the same oxygen isotope signature or be an indication that the fluid(s) underwent isotopic exchange with host Wernecke Supergroup sedimentary rocks (e.g., Sheppard 1986; Ohmoto 1986). It is not pos-

sible to differentiate between the two scenarios, however, isotopic information from the Slab prospect suggests fluid–rock interaction may have been significant. In the Slab area limestone layers in Fairchild Lake Group have $\delta^{18}O$ values 6‰ to 10‰ lower than expected for Proterozoic rocks of similar age (Fig. 6; Table 2), suggesting interaction with a fluid that had a low $\delta^{18}O$ value, such as meteoric, seawater, or formational water.

Discussion

Wernecke Breccia bodies and associated IOCG mineralization occur in areas underlain by Wernecke Supergroup sedimentary rocks that are up to 13 km thick (e.g., Thorkelson 2000; Thorkelson et al. 2001*a*; Hunt et al., 2005). The sedimentary strata have undergone greenschist-facies metamorphism and deformation. Mafic to intermediate Bonnet Plume River Intrusions are locally abundant in areas underlain by the Wernecke Supergroup and Wernecke Breccia and mafic to intermediate subaerial flows occur in the Slab area (Slab volcanics). This suggests that fluids associated with the breccia and mineralization could have had several sources, including meteoric water, seawater, water derived from diagenesis and compaction of basinal sediments (including evaporites), water derived from metamorphism of rocks of the Wernecke Supergroup, and magmatic water and (or) vapors. The following section reviews the available data and the constraints this data puts on fluid characteristics and possible fluid sources.

Constraints on fluid temperature, pressure, and composition

Oxygen isotopic values for coexisting dolomite and calcite from the Slab area indicate a temperature of ~300 °C, and at Igor, barite–chalcopyrite pairs indicate temperatures of ~240 and 350 °C (Table 6). These data were used in conjunction with fluid inclusion microthermometry data to estimate fluid pressure using the methods of Shepherd and Rankin (1998), the programme Flin-Calc, and the equations of Zhang and Frantz (1987) and Brown (1998). Results for the Slab area range from 2420 to 3000 bars, which, assuming lithostatic confining pressure and a rock density of 2.7 g/cm^3 (Shepherd et al. 1985), correspond to depths of ~9.1 to 11.3 km (Ta-Table 7). The results are similar to upper estimates for the combined thickness of Quartet Group and Gillespie Lake Group (7.4 to 9 km) that overlie the Slab prospect (Fig. 2; Delaney 1981; Thorkelson 2000). Results for Igor range from 1500 to 1900 bars, corresponding to depths of ~5.7 to 7.2 km. This depth range is in agreement with the >4 km estimated thickness for Quartet and Gillespie Lake Group strata that overlie the Igor prospect. The Hoover and Slats-Frosty prospects are overlain by ~7 to 9 km of Wernecke Supergroup strata and the Olympic prospect by 0.4 to 1.5 km (based on stratigraphic sections of Delaney 1981). The pressure estimates allow approximate fluid inclusion trapping temperatures to be calculated for the Hoover, Slats-Frosty, and Olympic areas. Using the upper limit of stratigraphic thickness on isochore diagrams gives average trapping temperatures of 285, 235, and 185 °C for syn-breccia fluids at Hoover, Slats-Frosty, and Olympic, respectively (Table 7).

Fluid inclusion data indicate that Wernecke Breccia formed from fluid(s) in a H_2O–NaCl–$CaCl_2$ + iron system. Evidence for this includes the occurrence of halite and hematite daughter phases and the presence of $CaCl_2$ in the fluid, as indicated by the formation of brown ice during freezing and initial melting temperatures below –50 °C (e.g., Potter et al. 1978, Vanko et al. 1988; Zwart and Touret 1994*)*. Preliminary proton induced X-ray emission (PIXE) data for fluid inclusions from Slab and Igor also indicate elevated levels of Cl, Na, and Ca ± Fe and Mn in the fluid (Gillen et al. 2004*b*).

The composition of fluid associated with brecciation and the isotopic compositions of minerals precipitated from it appear to be controlled, to some degree, by the composition of the host rocks. Na-rich, high-salinity fluids occur at the Slab prospect which is hosted in upper Fairchild Lake Group rocks that contain metaevaporites (Figs. 4, 5; Table 1; Hunt et al. 2005). Ca-rich, lower salinity fluids occur at the Olympic prospect, which occurs in Gillespie Lake Group dolostone. Fluids of varied composition and salinity occur between these two end-member types in prospects that are hosted by the Quartet Group. Lithological control on isotopic ratios is indicated by $\delta^{18}O$ values for the prospects that are similar to those of the host Wernecke Supergroup strata (Fig. 5). Carbon isotope results are also indicative of lithological control in that samples from veins hosted by carbonaceous shale have lower $\delta^{13}C$ values than those hosted by calcareous siltstone (Figs. 5*b*, 5*c*).

The fluid inclusion and isotopic data are also consistent with the composition of alteration assemblages that are associated with Wernecke Breccia. Alteration extends for metres to hundreds of metres beyond the breccias and varies from sodic- to potassic- to calcic-dominant as the lithology changes from Fairchild Lake Group to Quartet Group to Gillespie Lake Group (Hunt et al. 2005). However, at each prospect, syn- to post-breccia alteration and veining are dominated by carbonate. The type of carbonate also varies with host lithology. Calcite is dominant in the Slab and Hoover areas; dolomite and ankerite are dominant at Slats and Olympic. In the Igor prospect the late carbonate phase includes siderite, as well as dolomite, ankerite, and abundant barite.

Constraints from oxygen and hydrogen isotopes

Calculated values for water co-existing with syn-breccia muscovite, biotite, and actinolite in Wernecke Breccia have a wide range, especially in δD (–73‰ to +27‰; Fig. 7) and, thus, do not uniquely constrain the fluid source. The fluid may have been a mixture of waters from a number of sources.

The δD and $\delta^{18}O$ values of seawater are increased by evaporation (Fig. 7; Knauth and Beeunas 1986), which could account for the high δD_{water} values calculated from muscovite in Wernecke Breccia samples. Some of the high $\delta^{18}O$ values could be owing to exchange between seawater and ^{18}O-rich minerals, such as carbonates (Sheppard 1986). Mixing of this evolved seawater with variable amounts of low δD water (e.g., organic water) could produce the remainder of the depleted δD_{water} values seen. The evaporation of meteoric water can also lead to higher δD and $\delta^{18}O$ values, and its interaction with ^{18}O-rich minerals in the host rocks can lead to marked enrichment in ^{18}O relative to local meteoric water (Fig. 7; Sheppard 1986; cf., Salton Sea and Lanzarote areas).

Table 6. Estimates of fluid temperature determined from fluid inclusion and stable isotope data.

Prospect	Method	*T* (°C)
Slab	Fluid inclusion analyses	226–245[a]
Slab	$\delta^{18}O$: dolomite–calcite mineral pair	~300[b]
Hoover	Fluid inclusion analyses	153–188
Slats-Frosty	Fluid inclusion analyses	>160
Igor	Fluid inclusion analyses	220–250
Igor	$\delta^{34}S$: barite–chalcopyrite mineral pair	~350[c]
Olympic	Fluid inclusion analyses	158–170

[a]All direct fluid inclusion analyses are minimum temperatures, i.e., not trapped during phase separation.
[b]Using fractionation factors of Sheppard and Schwarcz (1970) and Golyshev et al. (1981).
[c]Using fractionation factors of Ohmoto and Lasaga (1982).

Table 7. Estimates of (1) thickness of strata overlying the IOCG prospects based on stratigraphic measurements (Delaney, 1981), (2) depth of the prospects based on pressure estimates, (3) pressure from fluid inclusion data, and (4) trapping temperature of fluid (see text for discussion).

Prospect	(1) Thickness (km)	(2) Depth (km)	(3) Pressure (kbar)	(4) Temperature (°C)
Slab	7.4–9.0	9.1–11.3	2.4–3.0	300
Hoover	7.0–9.0			285
Slats-Frosty	7.0–9.0			235
Igor	>4	5.7–7.2	1.5–1.9	350
Slats-Wallbanger	2.1–4.0			N/A
Olympic	0.4–1.5			185

N/A, not available. 1 kbar = 100 MPa.

In this case, the range in δD values could be because of mixing with variable amounts of low δD water and (or) evolved seawater. However, in general, the high salinity of Wernecke Breccia fluids is not consistent with a dominantly meteoric water source for the fluids.

Calculated δD_{water} and $\delta^{18}O_{water}$ values for Wernecke Breccia samples fall in the overlapping area between high-temperature formation waters (high $\delta^{18}O$ values) and metamorphic waters (Fig. 7). Thus, evolved formation waters would be consistent with most of the calculated isotopic ratios. Several of the samples have δD–$\delta^{18}O$ fluid values that fall within the magmatic fields on Fig. 7. However, these fields also lie within the overlapping area for formational and metamorphic waters. Magmatic waters are considered less likely to be a significant source of fluid than other sources because there are no magmatic rocks of appropriate age in the Wernecke area. The breccias are spatially associated with Bonnet Plume River Intrusions and the breccias contain clasts of the intrusive rocks, but the ca. 1600 Ma age of Wernecke Breccia rules out a genetic link between Bonnet Plume River Intrusions magmatism (ca. 1710 Ma) and brecciation–mineralization (Thorkelson et al. 2001*a* and 2001*b*). The age of the Slab volcanics is unknown, but they occur as clasts within Wernecke Breccia and so must also be older than the breccia (Thorkelson 2000). In addition, the Slab volcanics occur only locally at the eastern end of the breccia belt and, therefore, are unlikely to be related to brecciation that occurred over hundreds of kilometres. Nevertheless, the possibility of buried intrusion(s) beneath the Wernecke Supergroup cannot be ruled out.

Constraints from carbon isotopes

Dissolution of limestone and dolostone and oxidation of organic matter are possible sources of carbon for hydrothermally precipitated carbonates associated with Wernecke Breccia (e.g., Ohmoto and Rye 1979; Giuliani et al. 2000). Magmatic waters as a source are considered less likely for reasons already discussed. At high temperatures (>~200 °C), dissolution reactions should produce CO_2 that is isotopically similar to that of the original carbonate, whereas decarbonization reactions may produce ^{13}C-enriched CO_2 (Ohmoto and Rye 1979). Organic components in sediments typically have low $\delta^{13}C$ values (approximately –35‰ to –10‰), and oxidation of this material produces CO_2 with a similar isotopic composition (e.g., Ohmoto and Rye 1979; Ganor et al. 1994). The $\delta^{13}C$ values for carbonaceous shale in the Quartet Group range from –26.7‰ to –20.8‰. Calcite precipitated from the oxidation of this organic matter would have $\delta^{13}C$ values of –16.9‰ to –11.0‰ at Slab (300 °C), –16.5‰ to –10.6‰ at Hoover (285 °C), –14.9‰ to –9.0‰ at Slats-Frosty (235 °C), –18.1‰ to –12.2‰ at Igor (350 °C), and –12.9‰ to –7.0‰ at Olympic (185 °C), based on the fractionation factors of Chacko et al. (1991) for calcite–graphite. Measured $\delta^{13}C$ values for carbonates are higher than these values at all of the prospects (Table 2); thus, organic matter is unlikely to have been a significant source of carbon for the hydrothermal precipitates. However, low $\delta^{13}C$ values in veins that cut carbonaceous shale at the Hoover and Slats-Frosty prospects may have formed from fluid that contained minor amounts of carbon derived from organic matter in addition to carbon from limestone–dolostone sources.

Fig. 8. Oxygen fugacity versus sulfur fugacity diagram calculated at pressure (2500 bars) and temperature (300 °C) appropriate for Slab area fluids, showing that for the observed mineral assemblage to occur log fO_2 and log fS_2 values are limited to approximately –31 to –30 and –10 to –7, respectively. Equations used to define the mineral stability fields are listed in Appendix A. 1 kbar = 100 MPa.

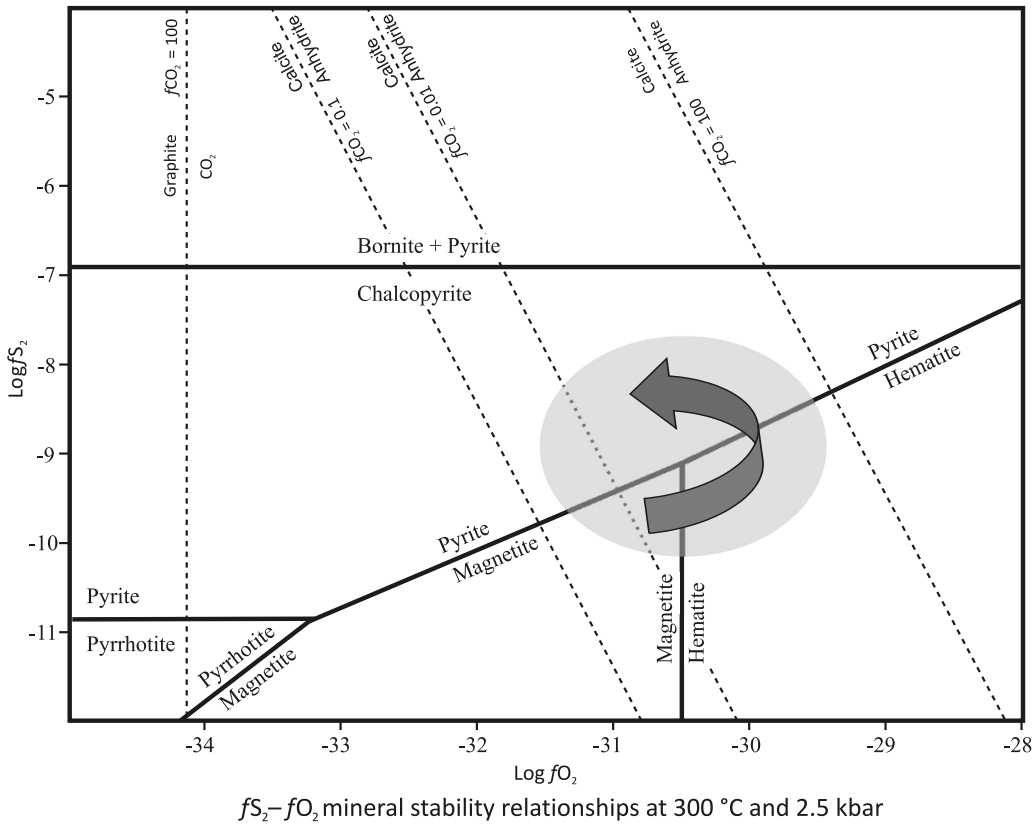

Calculated $\delta^{13}C$ values for carbonate precipitated from a 200 to 300 °C fluid that contained carbon derived by dissolution of Wernecke Supergroup limestone–dolostone range from –4.0‰ to 1.4‰ for calcite and –3.3‰ to –1.2‰ for dolomite, based on the fractionation factors for calcite-CO_2 and dolomite-CO_2 from Ohmoto and Rye (1979). The $\delta^{13}C$ values for hydrothermal carbonates from the prospects studied (Table 2) are similar to the calculated values, suggesting dissolution of carbonates was a possible source of carbon in the fluid. The influence of Wernecke Supergroup strata on the isotopic composition of the fluid is also reflected in the $\delta^{18}O$ results for the hydrothermal carbonates, which are similar to those of the host rocks (Fig. 5).

Constraints from sulfur isotopes

Sulfur in hydrothermally precipitated sulfide and sulfate minerals associated with Wernecke Breccia could have been derived from several sources including seawater, host sedimentary and igneous rocks, and magmatic fluids. A wide range of sulfur isotopic ratios was found in the prospects studied and no sulfur reservoir is clearly defined (Fig. 6). Values of $\delta^{34}S$ for pyrite that would have precipitated from the fluid in the Slab area can be estimated from Figs. 8, 9. In these breccias, magnetite is replaced by hematite but also occurs in minor amounts in later paragenetic stages (Hunt 2005). The hematite occurs with pyrite. Both are overprinted by chalcopyrite; pyrrhotite and bornite are not present. This assemblage indicates the oxygen and sulfur fugacity of the fluids changed through time but remained close to that of the magnetite–hematite–pyrite buffer assemblage. The presence of calcite and (or) ankerite, and the absence of graphite or anhydrite limits the log fCO_2 to >–1 and <2.

In Fig. 9, expected pyrite $\delta^{34}S$ values were calculated assuming the initial source of sulfur was (1) magmatic, with $\delta^{34}S$ = 0‰ (e.g., Ohmoto and Goldhaber 1997), and (2) Paleoproterozoic seawater, with $\delta^{34}S$ = 18‰ (Strauss 1993). Calculated $\delta^{34}S_{pyrite}$ values in equilibrium under conditions estimated for the Slab prospect (i.e., near magnetite–hematite–pyrite (mt–hem–py)) range from about –22‰ to –15‰ for a magmatic source of sulfur and from –3.4‰ to +3.6‰ for a seawater source of sulfur (Fig. 9). Measured sulfur isotope values for pyrite range from –5.8‰ to +7.1‰, similar to those calculated for a seawater source of sulfur or sediments–evaporite deposits precipitated from that seawater. The wide range of $\delta^{34}S$ values may be owing to small changes in fO_2 and (or) pH because fluid conditions occur where the $\delta^{34}S$ contours are close together (Fig. 9). Variability in $\delta^{34}S$ values from the Hoover, Slats, Igor, and Olympic prospects may also be owing to changes in fO_2 or pH in the hydrothermal fluids, but further data is required to determine this.

Conclusions

Fluid inclusion analyses of Wernecke Breccia samples allowed the estimation of pressure–temperature–composition (*P*–*T*–*X*) characteristics for the breccia forming-IOCG mineralizing fluids. Estimates of fluid pressure determined from

Fig. 9. Approximate breccia-forming–mineralizing fluid conditions at the Slab prospect (shaded area) in pH versus oxygen fugacity space. The positions of δS^{34}_i contours are also shown. Numbers in boxes on contours are δS^{34}_{pyrite} values calculated using $\delta S^{34}_{\Sigma S}$ = 0‰ (right side) and $\delta S^{34}_{\Sigma S}$ = 18‰ (left side). Positions of sulfur isotope contours were calculated using the methods described in detail in Ohmoto (1972) with the following conditions: temperature = 300 °C, pressure = 2500 bars, ionic strength = 3.2 (based on fluid inclusion data), log fO_2 = –31.24, log fS_2 = –8.5, log aH_2S = –2.6 (fixed sulfur concentration = 0.0032 molality), pH = 5. Species calculated to be most abundant in the fluid are listed in Appendix A. 1 bar = 100 kPa.

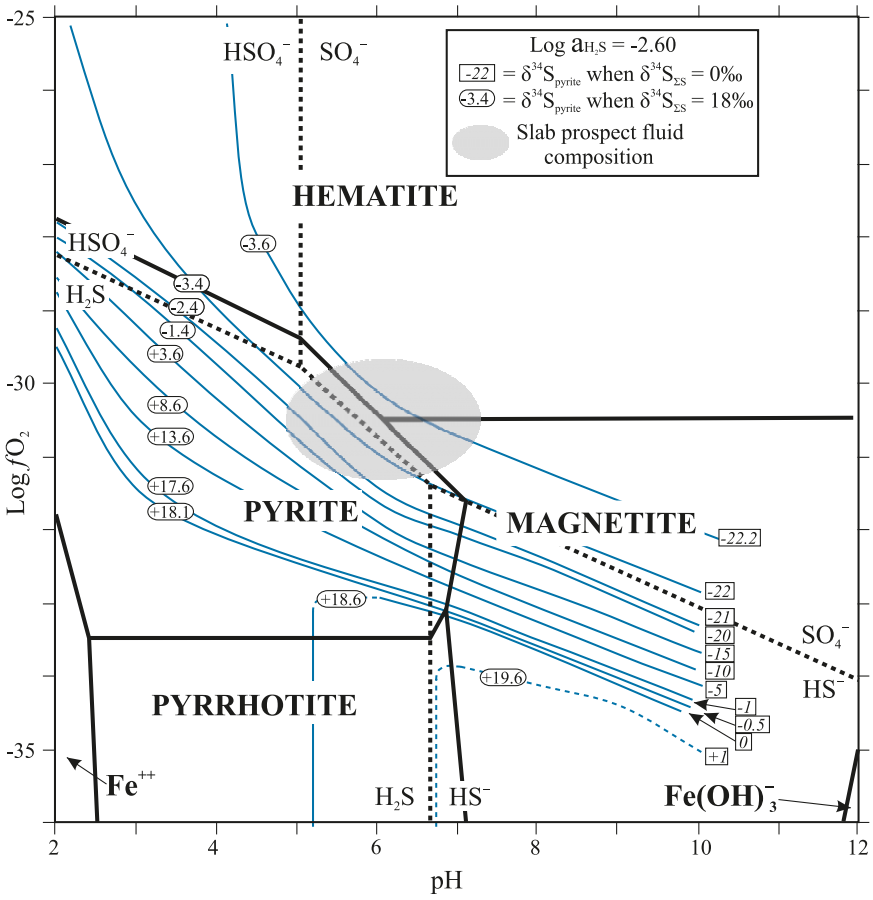

fluid inclusion data are in reasonable agreement with those based on the thickness of overlying stratigraphy and vary from ~0.4 to 2.4 kbar. Pressure adjusted fluid temperatures range from about 185 to 350 °C (Table 7). Mineral assemblages and crosscutting relationships observed at all of the IOCG prospects indicate fluid conditions were close to the magnetite–hematite–pyrite triple junction during brecciation. The fluids are high salinity (24–42 wt.% NaCl equiv.) NaCl–$CaCl_2$–H_2O brines with compositions that appear to reflect significant interaction with the host strata. For example, at the Slab prospect that is hosted by upper Fairchild Lake Group that contains metaevaporites (metahalite facies), the fluids are dominated by Na. Fluids at the Olympic prospect, which is hosted by Gillespie Lake Group dolostone, are dominated by Ca.

Hydrogen isotope data indicate the source of fluids that formed Wernecke Breccia and associated IOCG mineralization was most likely formational/metamorphic water mixed with variable amounts of low δD (e.g., organic) water ± evolved meteoric water and (or) evolved seawater (Fig. 8). The $\delta^{13}C$ values of hydrothermal carbonates indicate the carbon was derived in large part from the host Wernecke Supergroup (Fig. 5; Table 2). The $\delta^{34}S$ values of hydrothermal pyrite, chalcopyrite, and barite point to seawater (or sediments/evaporites deposited from seawater) as a likely source for much of the sulfur (Fig. 9), with possible additional sources from the leaching of biogenic pyrite and (or) sulfides in local igneous rocks (Bonnet Plume River Intrusions and (or) Slab volcanics). The high salinity of the fluid is consistent with derivation from an evaporite-bearing sedimentary sequence deposited at a continental margin (Yardley and Graham 2002).

Halogen and noble gas data reported by Kendrick et al., (2008) for the six Wernecke Breccia prospects also support a dominantly sedimentary source for breccia-mineralizing fluid. The halogen data suggest fluid interaction with halite (or scapolite) has enhanced the fluid salinity, particularly in the Slab area. The noble gas data indicate the significant involvement of sedimentary formation water in all of the prospects, i.e., a fluid with a significant noble gas concentration and low $^{40}Ar/^{36}Ar$ values. However, results returned by samples from Igor, Olympic, and Hoover also suggest the involvement of another fluid with low noble gas concentration, high $^{40}Ar/^{36}Ar$ values, and a crustal He and Ne isotope signature. Kendrick et al. (2008) suggest this fluid is likely to be basement derived and could have been generated by metamorphic devolatiliza-

tion or by exsolving a magmatic fluid from melts formed during crustal anatexis, or both processes concurrently. They state that the noble gas data preclude a direct link to mantle-derived magmatism.

Taken together these results suggest fluid that formed Wernecke Breccia and associated IOCG mineralization was dominantly formation/metamorphic water that may have been mixed with minor amounts of other waters. This is similar to the evaporitic-source model proposed by Barton and Johnson (1996, 2000). The Wernecke Breccias have features indicative of an "evaporitic component", i.e., direct association with an evaporite-bearing basin, voluminous sodic alteration, and geochemical data that point to fluids that are dominantly non-magmatic. In Barton and Johnson's (1996, 2000) model evaporitic sources provide the chloride necessary for the transport of metals that are derived from igneous rocks. The source of metals in Wernecke Breccia fluids is unknown, but it may have been derived from the host rocks. Whole-rock analyses indicate that the lower and middle parts of the Wernecke Supergroup (i.e., Fairchild Lake Group and Quartet Group) contain elevated levels of Cu, U, and Co; mafic to intermediate Bonnet Plume River Intrusions and (or) the Slab volcanics locally contain disseminated chalcopyrite and (or) malachite (Goodfellow 1979; Lane 1990; Thorkelson 2000). Thus, fluid could have leached metals from the host strata.

The Barton and Johnson (1996, 2000) model invokes magmatism as the source of heat to drive fluid circulation and generate the required high temperatures. This is problematic in the Wernecke Mountains where no intrusive rocks of appropriate age are known. Previous authors (see Thorkelson 2000 for a review) have suggested buried intrusive as the source of heat. Kendrick et al. (2008) suggest a deep-seated regional thermal disturbance may have been responsible, based on their noble gas data. Another possible solution that would form fluids with the required high temperatures is to use a simple burial model. An average geothermal gradient of 25–30 °C/km (e.g., Raymond 1995, 2000) and a surface temperature of 25 °C would produce temperatures of 250 to 295 °C at depths of 7 to 9 km. The geothermal gradient may have been higher than average in the Wernecke Mountains area because it is postulated to have been a rifting/extensional environment during deposition of Wernecke Supergroup and emplacement of Bonnet Plume River Intrusions (Thorkelson 2000; Thorkelson et al. 2001*a*). The Wernecke Breccias were formed syn- to post-deformation (Hunt et al. 2005), thus fluid circulation could have been driven by tectonic processes.

Constrained by these new geochemical parameters, the genesis of Wernecke Breccia and associated IOCG mineralization appears to be strongly related to the temporal evolution of the sedimentary basin. High salinity brines, formed in part from the dissolution of evaporites, could have been driven by deformation (± deep-seated heat) and mobilized mineralizing components from the enclosing rocks. The emerging hypothesis is that periodic (tectonic–stratigraphic) over-pressuring of the fluids led to repeated brecciation and mineral precipitation within hydraulic breccias, vein networks, and disseminations.

If, as is indicated by the new fluid data, Wernecke Breccia-related IOCG mineralization is largely independent of magmatism, this has implications in the search for IOCG deposits on a broader scale. Traditionally, exploration for IOCG deposits has focused on areas where brecciation is temporally related to magmatism (with proximal or distal intrusive rocks). However, the new information obtained from Wernecke Breccia suggests IOCG mineralization may also be found in thick sedimentary sequences (i.e., either thick enough to produce high temperature basinal fluids or an area of higher than average heat flow) that contain sources of metals (host sedimentary or igneous rocks), a source of chloride for metal transport (e.g., evaporites), traps for metal precipitation (e.g., breccia zones), plus a mechanism to drive fluid flow (e.g., tectonics, gravity).

Acknowledgements

Support for this project was provided by the Yukon Geological Survey, an Australian International Postgraduate Research Scholarship, a James Cook University scholarship and Merit Research Grant, a Society of Economic Geologists Student Research Grant, and a predictive minerals discovery* Cooperative Research Centre scholarship. Newmont Mining Corporation, Archer, Cathro & Associates (1981) Ltd., Equity Engineering, Pamicon Developments, Monster Copper Resources, and Blackstone Resources kindly provided access to confidential data, drill core, and (or) properties. The manuscript benefitted from reviews and comments by Murray Hitzman, Martin Smith, James Mortensen, David Huston, Mark Hannington and editorial staff.

References

Archer, A.R., and Schmidt, U. 1978. Mineralised breccias of early Proterozoic age, Bonnet Plume River District, Yukon Territory. CIM Bulletin, **71**: 53–58.

Archer, A., Bell, R.T., Delaney, G.D., and Godwin, C.I. 1977. Mineralized breccias of Wernecke Mountains Yukon. Geological Association of Canada, Program with Abstracts, **2**: 5.

Barton, M.D., and Johnson, D.A. 1996. Evaporitic-source model for igneous-related Fe oxide – (REE–Cu–Au–U) mineralization. Geology, **24**(3): 259–262. doi:10.1130/0091-7613(1996)024<0259:ESMFIR>2.3.CO;2.

Barton, M.D., and Johnson, D.A. 2000. Alternative brine sources for Fe-Oxide(–Cu–Au) systems: implications for hydrothermal alteration and metals. *In* Hydrothermal iron oxide copper–gold & related deposits: a global perspective. *Edited by* T.M. Porter. Vol. 1. PGC Publishing, Adelaide, Australia. pp. 43–60.

Bastrakov, E.N., Shvarov, Y.V., Girvan, S., Cleverley, J.S., and Wyborn, L. 2004. FreeGs: web-enabled thermodynamic database for modelling of geochemical processes. *In* Dynamic Earth: past, present and future: abstracts of the 17th Australian Geological Convention, Hobart, Tasmania, Australia, February 8–13. *Edited by* J. McPhie and P. McGoldrick. pp. 10–15.

Beaudoin, G., and Therrien, P. 2008. Stable isotope fractionation calculator (http://www2.ggl.ulaval.ca/cgi-bin/isotope/generisotope.cgi/) (accessed August 2011).

Bell, R.T. 1978. Breccias and uranium mineralization in the Wernecke Mountains, Yukon Territory — a progress report. *In* Current research, part A. Geological Survey of Canada, Paper 78-1A. pp. 317–322.

Bell, R.T. 1986*a*. Megabreccias in northeastern Wernecke Mountains, Yukon Territory. *In* Current research, part A. Geological Survey of Canada, Paper 86-1A. pp. 375–384.

Bell, R.T. 1986*b*. Geological map of north-eastern Wernecke

Mountains, Yukon Territory. Geological Survey of Canada, Open File Map 1027, scale 1 : 250 000.

Bell, R.T., and Delaney, G.D. 1977. Geology of some uranium occurrences in Yukon Territory. *In* Report of activities, part A. Geological Survey of Canada, Paper 77-1A. pp. 33–37.

Bethke, C. 2002. The Geochemist's Workbench Version 4.0: A users guide. University of Illinois, Urbana, Ill., USA. 100 p.

Brideau, M.-A., Thorkelson, D.J., Godin, L., and Laughton, J.R. 2002. Paleoproterozoic deformation of the Racklan Orogeny, Slats Creek and Fairchild Lake map areas, Wernecke Mountains, Yukon. *In* Yukon exploration and geology 2001. *Edited by* D.S. Emond, L.H. Weston, and L.L. Lewis. Exploration and Geological Services Division, Yukon Region, Indian and Northern Affairs Canada. pp. 65–72.

Brown, P.E. 1998. Fluid inclusion modeling for hydrothermal systems. *In* Techniques in hydrothermal ore deposits geology. *Edited by* J.P. Richards and P.B. Larson. Reviews in Economic Geology 10. pp. 151–171.

Chacko, T., Mayeda, T.K., Clayton, R.N., and Goldsmith, J.R. 1991. Oxygen and carbon isotope fractionations between CO_2 and calcite. Geochimica et Cosmochimica Acta, **55**(10): 2867–2882. doi:10.1016/0016-7037(91)90452-B.

Cleverley, J.S., and Bastrakov, E.N. 2005. K2GWB: Utility for generating thermodynamic data files for The Geochemist's Workbench (R) at 0–1000 °C and 1–5000 bars from UT2K and the UNITHERM database. Computers & Geosciences, **31**(6): 756–767. doi:10.1016/j.cageo.2005.01.007.

Delaney, G.D. 1981. The Mid-Proterozoic Wernecke Supergroup, Wernecke Mountains, Yukon Territory. *In* Proterozoic basins of Canada. Geological Survey of Canada, Paper 81-10. pp. 1–23.

Donnelly, T., Waldron, S., Tait, A., Dougans, J., and Bearhop, S. 2001. Hydrogen isotope analysis of natural abundance and deuterium-enriched waters by reduction over chromium on-line to a dynamic dual inlet isotope-ratio mass spectrometer. Rapid Communications in Mass Spectrometry, **15**(15): 1297–1303. doi:10.1002/rcm.361. PMID:11466788.

Fallick, A.E., Macauley, C.I., and Haszeldine, R.S. 1993. Implications of linearly correlated oxygen and hydrogen isotopic compositions for kaolinite and illite in the magnus sandstone, North Sea. Clays and Clay Minerals, **41**(2): 184–190. doi:10.1346/CCMN.1993.0410207.

Furlanetto, F., Thorkelson, D.J., Davis, W.J., Gibson, H.D., Rainbird, R.H., and Marshall, D.D. 2009. Preliminary results of detrital zircon geochronology, Wernecke Supergroup, Yukon. *In* Yukon exploration and geology 2008. *Edited by* L.H. Weston, L.R. Blackburn, and L.L. Lewis. Yukon Geological Survey. pp. 125–135.

Gabrielse, H. 1967. Tectonic evolution of the northern Canadian Cordillera. Canadian Journal of Earth Sciences, **4**(2): 271–298. doi:10.1139/e67-013.

Ganor, J., Matthews, A., and Schliestedt, M. 1994. Post-metamorphic low $\delta^{13}C$ in the Cycladic complex (Greece) and their implications for modelling fluid infiltration processes using carbon isotope compositions. European Journal of Mineralogy, **6**: 365–379.

Gillen, D., Baker, T., and Hunt, J.A. 2004*a*. Fluid inclusion studies in Fe-oxide Cu-Au deposits, Wernecke Mountains. *In* Dynamic Earth: past, present and future.17th Australian Geological Convention, Hobart, Australia. *Edited by* J. McPhie, and P. McGoldrick. Geological Society of Australia, Abstracts 73. p. 82.

Gillen, D., Baker, T., Hunt, J.A., Ryan, C., and Win, T.T. 2004*b*. PIXE analysis of hydrothermal fluids in the Wernecke Mountains, Canada. *In* Predictive mineral discovery CRC conference: focus on science, Barossa Valley, 1–3 June. *Edited by* A.C. Barnicoat and R.J. Korsch. Extended Abstracts. pp. 69–73.

Giuliani, G., France-Lanford, C., Cheilletz, A., Coget, P., Branquet, Y., and Laumomnier, B. 2000. Sulfate reduction by organic matter in Colombian Emerald deposits: chemical and stable isotope (C,O, H) evidence. Economic Geology and the Bulletin of the Society of Economic Geologists, **95**(5): 1129–1153. doi:10.2113/95.5.1129.

Goldstein, R.H., and Reynolds, T.J. 1994. Systematics of fluid inclusions in diagenetic minerals. Society for Sedimentary Geology, Short Course 31. 199 p.

Golyshev, S.I., Padalko, N.L., and Pechenkin, S.A. 1981. Fractionation of stable oxygen and carbon isotopes in carbonate systems. Geochemistry International, **18**: 85–99.

Goodfellow, W.D. 1979. Geochemistry of copper, lead and zinc mineralization in Proterozoic rocks near Gillespie Lake, Yukon. *In* Geological Survey of Canada, Paper 79-1A. pp. 333–348.

Graham, C.M., Harmon, R.S., and Sheppard, S.M.F. 1984. Experimental hydrogen isotope exchange between amphibole and water. The American Mineralogist, **69**: 128–138.

Hitzman, M.W. 2000. Iron oxide – Cu–Au deposits: what, where, when, and why? *In* Hydrothermal iron oxide copper–gold & related deposits: a global perspective. *Edited by* T.M. Porter. PGC Publishing, Adelaide, Australia. Vol. 1. pp. 9–25.

Hitzman, M.W., Oreskes, N., and Einaudi, M.T. 1992. Geological characteristics and tectonic setting of Proterozoic iron oxide (Cu–U–Au–REE) deposits. Precambrian Research, **58**(1–4): 241–287. doi:10.1016/0301-9268(92)90121-4.

Hunt, J.A. 2005. The geology and genesis of iron oxide – copper–gold mineralisation associated with Wernecke Breccia, Yukon, Canada. Unpublished Ph.D. thesis, James Cook University, Townsville, Australia. 125 p.

Hunt, J.A., Laughton, J.R., Brideau, M.-A., Thorkelson, D.J., Brookes, M.L., and Baker, T. 2002. New mapping around the Slab iron oxide – copper–gold occurrence, Wernecke Mountains. *In* Yukon exploration and geology 2001. *Edited by* D.S. Emond, L.H. Weston, and L.L. Lewis. Exploration and Geological Services Division, Yukon Region, Indian and Northern Affairs Canada. pp. 125–138.

Hunt, J.A., Baker, T., and Thorkelson, D.J. 2005. Regional-scale Proterozoic IOCG-mineralised breccia systems: examples from the Wernecke Mountains, Yukon, Canada. Mineralium Deposita, **40**(5): 492–514. doi:10.1007/s00126-005-0019-5.

Kendrick, M.A., Honda, M., Gillen, D., Baker, T., and Phillips, D. 2008. New constraints on regional brecciation on the Wernecke Mountains, Canada, from He, Ne, Ar, Kr, Xe, Cl, Br and I. Chemical Geology, **255**(1–2): 33–46. doi:10.1016/j.chemgeo.2008.05.021.

Knauth, L.P., and Beeunas, M.A. 1986. Isotope geochemistry of fluid inclusions in Permian halite with implications for the isotopic history of ocean water and the origin of saline formation waters. Geochimica et Cosmochimica Acta, **50**(3): 419–433. doi:10.1016/0016-7037(86)90195-X.

Lane, R.A. 1990. Geologic setting and petrology of the Proterozoic Ogilvie Mountains breccia of the Coal Creek Inlier, southern Ogilvie Mountains, Yukon Territory. Unpublised M.Sc. thesis, The University of British Columbia, Vancouver, B.C., Canada. 223 p.

Laughton, J.R. 2004. The Proterozoic Slab volcanics of northern Yukon, Canada: megaclasts of a volcanic succession in Proterozoic Wernecke Breccia, and implications for the evolution of northwestern Laurentia. Unpublished M.Sc. thesis, Simon Fraser University, Burnaby, B.C., Canada. 123 p.

McCrea, J.M. 1950. On the isotopic chemistry of carbonates and a paleotemperature scale. Journal of Chemical Physics, **18**(6): 849–857.

Norris, D.K. 1997. Geology and mineral and hydrocarbon potential of northern Yukon Territory and northwestern district of Mackenzie. Geological Survey of Canada, Bulletin 422. 401 p.

Ohmoto, H. 1972. Systematics of sulfur and carbon isotopes in hydrothermal ore deposits. Economic Geology, **67**(5): 551–578. doi:10.2113/gsecongeo.67.5.551.

Ohmoto, H. 1986. Stable isotope geochemistry of ore deposits. *In* Stable isotopes in high temperature geological processes. *Edited by* J.W. Valley, H.P. Taylor Jr., and J.R. O'Neil. Mineralogical Society of America, Reviews in Mineralogy, Vol. 16. pp. 491–559.

Ohmoto, H., and Goldhaber, M.B. 1997. Sulfur and carbon isotopes. *In* Geochemistry of hydrothermal ore deposits. *Edited by* H.L. Barnes. John Wiley and Sons, New York, N.Y., USA. pp. 517–612.

Ohmoto, H., and Lasaga, A.C. 1982. Kinetics of reactions between aqueous sulfates and sulfides in hydrothermal systems. Geochimica et Cosmochimica Acta, **46**(10): 1727–1745. doi:10.1016/0016-7037(82)90113-2.

Ohmoto, H., and Rye, R.O. 1979. Isotopes of sulfur and carbon. *In* Geochemistry of hydrothermal ore deposits. *Edited by* H.L. Barnes. John Wiley & Sons, New York, N.Y. pp. 509–567.

Potter, R.W., Clynne, M.A., and Brown, D.L. 1978. Freezing point depression of aqueous sodium chloride solutions. Economic Geology, **73**(2): 284–285. doi:10.2113/gsecongeo.73.2.284.

Raymond, J. 1995. Petrology: The study of igneous, metamorphic and sedimentary rocks. McGraw-Hill Higher Education, New York, N.Y. 742 p.

Raymond, J. 2000. Mantle of the earth. *In* Encyclopedia of volcanoes. *Edited by* H. Sigurdsson. Academic Press, San Diego, Calif., USA. pp. 41–54.

Reynolds, L.J. 2000. Geology of the Olympic Dam Cu–U–Au–Ag–REE deposit. *In* Hydrothermal iron oxide – copper–gold & related deposits: a global perspective. *Edited by* T.M. Porter. PGC Publishing, Adelaide, Australia. Vol. 1. pp. 93–104.

Robinson, B.W., and Kusakabe, M. 1975. Quantitative preparation of sulfur dioxide, for sulfur-34/sulfur-32 analyses, from sulfides by combustion with cuprous oxide. Analytical Chemistry, **47**(7): 1179–1181. doi:10.1021/ac60357a026.

Roedder, E. 1984. Fluid inclusions. Reviews in Mineralogy, Vol. 12. 644 p.

Rollinson, H. 1993. Using geochemical data: evaluation, presentation, interpretation. Longman Group, UK. 352 p.

Ryan, A. 1998. Ernest Henry copper–gold deposit. *In* Geology of Australian and Papua New Guinean mineral deposits. *Edited by* D. A. Berkman and D.H. Mackenzie. Australasian Institute of Mining and Metallurgy, Melbourne, Australia, Monograph 22. pp. 759–768.

Rye, R.O., and Ohmoto, H. 1974. Sulfur and carbon isotopes and ore genesis: a review. Economic Geology, **69**(6): 826–842. doi:10.2113/gsecongeo.69.6.826.

Sharp, Z.D. 1990. A laser-based microanalytical method for the in situ determination of oxygen isotope ratios in silicates and oxides. Geochimica et Cosmochimica Acta, **54**(5): 1353–1357. doi:10.1016/0016-7037(90)90160-M.

Shepherd, T.J., and Rankin, A.H. 1998. Fluid inclusion techniques of analysis. *In* Techniques in hydrothermal ore deposits geology. *Edited by* J.P. Richards and P.B. Larsen. Society of Economic Geologists, Reviews in Economic Geology, Vol. 10. pp. 125–150.

Shepherd, T.J., Rankin, A.H., and Alderton, D.H.M. 1985. A practical guide to fluid inclusion studies. Blackie & Son Limited, Glasgow, Scotland. 200 p.

Sheppard, S.M.F. 1986. Characterization and isotopic variations in natural waters. *In* Stable isotopes in high temperature geological processes. *Edited by* Valley, J.W., Taylor, H.P. Jr., and O'Neil, J.R. Mineralogical Society of America, Reviews in Mineralogy, Vol. 16. pp. 165–183.

Sheppard, S.M.F., and Schwarcz, H.P. 1970. Fractionation of carbon and oxygen isotopes and magnesium between coexisting metamorphic calcite and dolomite. Contributions to Mineralogy and Petrology, **26**(3): 161–198. doi:10.1007/BF00373200.

Shields, G., and Veizer, J. 2002. Precambrian marine carbonate isotope database: version 1.1. Geochemistry Geophysics Geosystems, **3**(6): 1031 . [An electronic journal of the earth sciences published by AGU and the Geochemical Society.] doi:10.1029/2001GC000266.

Sillitoe, R.H. 2003. Iron oxide copper–gold deposits: an Andean view. Mineralium Deposita, **38**(7): 787–812. doi:10.1007/s00126-003-0379-7.

Strauss, H. 1993. The sulfur isotope record of Precambrian sulfates: new data and a critical evaluation of the existing record. Precambrian Research, **63**(3–4): 225–246. doi:10.1016/0301-9268(93)90035-Z.

Suzuoki, T., and Epstein, S. 1976. Hydrogen isotope fractionation between OH-bearing minerals and water. Geochimica et Cosmochimica Acta, **40**(10): 1229–1240. doi:10.1016/0016-7037(76)90158-7.

Thorkelson, D.J. 2000. Geology and mineral occurrences of the Slats Creek, Fairchild Lake and "Dolores Creek" areas, Wernecke Mountains, Yukon Territory. Exploration and Geological Services Division, Yukon Region, Indian and Northern Affairs Canada, Bulletin 10. 73 p.

Thorkelson, D.J., Mortensen, J.K., Creaser, R.A., Davidson, G.J., and Abbott, J.G. 2001*a*. Early Proterozoic magmatism in Yukon, Canada: constraints on the evolution of northwestern Laurentia. Canadian Journal of Earth Sciences, **38**(10): 1479–1494. doi:10.1139/e01-032.

Thorkelson, D.J., Mortensen, J.K., Davidson, G.J., Creaser, R.A., Perez, W.A., and Abbott, J.G. 2001*b*. Early Mesoproterozoic intrusive breccias in Yukon, Canada: The role of hydrothermal systems in reconstructions of North America and Australia. Precambrian Research, **111**(1–4): 31–55. doi:10.1016/S0301-9268(01)00155-3.

Thorkelson, D.J., Laughton, J.R., Hunt, J.A., and Baker, T. 2003. Geology and mineral occurrences of the Quartet Lakes map area, Wernecke and Mackenzie mountains, Yukon. *In* Yukon exploration and geology 2002. *Edited by* D.S. Emond and L.L. Lewis. Exploration and Geological Services Division, Yukon Region, Indian and Northern Affairs Canada. pp.223–239.

Valley, J.W., Taylor, H.P., Jr., and O'Neil, J.R. 1986. Stable isotopes in high temperature geological processes. Mineralogical Society of America, Reviews in Mineralogy, Vol. 16. 570 p.

Vanko, D.A., Bodnar, R.J., and Sterner, S.M. 1988. Synthetic fluid inclusions: VIII. Vapor-saturated halite solubility in part of the system NaCl–$CaCl_2$–H_2O, with application to fluid inclusions from oceanic hydrothermal systems. Geochimica et Cosmochimica Acta, **52**(10): 2451–2456. doi:10.1016/0016-7037(88)90303-1.

Yardley, B.W.D., and Graham, J.T. 2002. The origins of salinity in metamorphic fluids. Geofluids, **2**(4): 249–256. doi:10.1046/j.1468-8123.2002.00042.x.

Yukon MINFILE. 2008. Database of Yukon mineral occurrences. Exploration and Geological Services Division, Yukon Region, Indian and Northern Affairs Canada. [2 CD-ROMs.]

Zhang, Y.-G., and Frantz, J.D. 1987. Determination of the compositional limits of immiscibility in H_2O–CO_2–$CaCl_2$ fluids to 600 °C and 2.0 kbar using synthetic fluid inclusions. EOS, Transactions of the American Geophysical Union, **68**(44): 1539.

Zheng, Y.F. 1993. Calculation of oxygen isotope fractionation in hydroxyl-bearing silicates. Earth and Planetary Science Letters, **120**(3–4): 247–263. doi:10.1016/0012-821X(93)90243-3.

Zheng, Y.F. 1999. Oxygen isotope fractionation in carbonate and sulfate minerals. Geochemical Journal, **33**: 109–126.

Zwart, E.W., and Touret, J.L.R. 1994. Melting behaviour and composition of aqueous fluid inclusions in fluorite and calcite: applications within the system H_2O–$CaCl_2$–NaCl. European Journal of Mineralogy, **6**: 773–786.

Table A1. Equations used to define the mineral stability fields shown in Fig. 8.

Reaction used	Equation	Log K
Pyrite–magnetite:	$3\ FeS_2 + 2\ O_2(g) = Fe_3O_4 + 3\ S_2(g)$	–4.6
Pyrite–hematite:	$4\ FeS_2 + 3\ O_2(g) = 2\ Fe_2O_3 + 4\ S_2\ (g)$	33.88
Pyrrhotite–magnetite:	$6\ FeS + 4\ O_2(g) = 2\ Fe_3O_4 + 3\ S_2$	55.34
Bornite–chalcopyrite:	$Cu_5FeS_4 + 4\ FeS_2 = 5\ CuFeS_2 + S_2$	83.64
Graphite–CO_2(g):	$C + O_2(g) = CO_2(g)$	–6.93
Calcite–gypsum:	$2\ CaCO_3 + S_2(g) + 3\ O_2(g) + 4\ H_2O = 2\ CaSO_4 + 2\ CO_2(g)$	36.13

Note: g, gas.

Appendix A

Equations used to define the mineral stability fields shown in Fig. 8 are listed in Table A1. The most abundant species calculated to be in the Slab area fluid are listed in Table A2. Calculations were carried out using the software "The Geochemists Workbench"® release 4.0.2 (Bethke 2002). A recalculated database was used following the procedure of Cleverley and Bastrakov (2005) and using K2GWB software. The thermodynamic data was calculated at the conditions of interest, 2500 bars (1 bar = 100 kPa) and 300 °C, and was derived from the Geoscience Australia version of the UNITHERM database for the HCh package for geochemical modelling available through the "FreeGs" online database (Bastrakov et al. 2004).

Table A2. Calculations indicate the following species were most abundant in the Slab area fluid as shown in Fig. 9.

Species	Molality	Mole fraction
$NaSO_4^-$	0.6985	0.497
$CaSO_4$(aq)	0.3741	0.266
KSO_4^-	0.165	0.117
SO_4^-	0.1623	0.115
H_2S(aq)	2.51E-03	0.002
HSO_4^-	1.54E-03	0.001
HS^-	1.30E-03	0.001

Note: aq, aqueous.